A hypersingular boundary integral analysis of axisymmetric steady-state heat conduction across a non-ideal interface between two dissimilar materials*

E. L. Chen, W. T. Ang** and H. Fan
Division of Engineering Mechanics
School of Mechanical and Aerospace Engineering
Nanyang Technological University
Singapore 639798

Abstract

Steady-state axisymmetric heat conduction across a non-ideal interface between two dissimilar materials is considered. The non-ideal interface may be either low or high conducting. The relevant interfacial conditions are formulated in terms of hypersingular boundary integral equations. A simple boundary element procedure based on the hypersingular boundary integral formulations is proposed for solving numerically the axisymetric heat conduction problem under consideration. Numerical results for some specific problems are obtained.

Keywords: axisymmetric heat conduction, boundary integral method, bimaterial, non-ideal interface

* This is a preprint of the article published in:
Engineering Analysis with Boundary Elements
35 (2011) 1090-1100

** Corresponding author (mwtang@ntu.edu.sg)

1 Introduction

If two dissimilar materials are bonded together with a very thin layer of material sandwiched in between them, the layer may be modeled as an interface in the form of a line (for plane problems) or a surface (in the case of three-dimensional problems). The boundary conditions to impose on the line or surface interface depend on the properties of the material in the thin layer and may be derived using asymptotic analysis (see, for example, Benveniste and Miloh [5]). Such a line or surface interface model helps to simplify the mathematics involved in the analysis of the multi-layered material.

In the context of heat conduction theory, the line or surface interface is regarded as thermally low conducting if the thin layer is occupied by a material of extremely low thermal conductivity. As an example, the interface between two imperfectly joined materials, which contains microscopic gaps filled with air, may be modeled as low conducting. On the other hand, if a material of extremely high thermal conductivity occupies the thin layer, the interface is said to be thermally high conducting. In a thermal system comprising a computer chip and a heat sink, the interface between the two components (the chip and the sink) may be modeled as high conducting if they are joined together by a thin layer of carbon nanotubes (Desai, Geer and Sammakia [7]).

Interfacial conditions for thermally non-ideal interfaces that are either low or high conducting are given in Benveniste [4] and Miloh and Benveniste [8]. As one may intuitively expect, the temperature field varies continuously across a high conducting interface but it exhibits a jump across a low conducting interface. The normal heat flux is continuous on a low conducting interface but not on a high conducting one. The temperature jump across a low conducting interface is proportional in magnitude to the normal heat flux on the interface. For a high conducting interface, the jump in the normal heat flux is expressed in terms of second order spatial derivatives of the temperature on the interface.

To obtain a boundary element method for analyzing the two-dimensional steady-state temperature distribution in a bimaterial with a straight imperfect (low conducting) interface, Ang, Choo and Fan [2] have derived a Green's function that satisfies appropriate conditions on the interface be-

tween two dissimilar half-spaces. A hypersingular boundary integral formulation is given by Ang [1] for two-dimensional heat conduction across an arbitrarily curved low conducting interface in a bimaterial.

The analysis in [1] is extended here to derive a hypersingular boundary integral formulation for axisymmetric steady-state heat conduction across a curved low conducting interface in a bimaterial. Moreover, the case of a high conducting interface is considered here. The extension is by no means trivial, as the fundamental solution of the axisymmetric heat equation is rather complicated being expressed in terms of the complete elliptic integrals of the first and second kind. Together with the boundary integral equation for axisymmetric heat conduction, the hypersingular boundary integral formulation for each of the two types of interfaces is used to derive a simple boundary element procedure for computing numerically the temperature distribution in the bimaterial. The boundary element procedure is applied to solve some particular problems involving axisymmetric heat conduction in bimaterials with either low conducting or high conducting interfaces.

2 The problem

Consider a bimaterial comprising regions R_1 and R_2 which have thermal conductivities κ_1 and κ_2 respectively. With reference to a Cartesian coordinate system denoted by $Oxyz$, the regions R_1 and R_2 are symmetrical about the z-axis, that is, the regions R_1 and R_2 can be respectively obtained by rotating two-dimensional regions Ω_1 and Ω_2 on the rz (axisymmetric coordinate) plane by an angle of $360^{\rm o}$ about the z-axis. (Note that $r = \sqrt{x^2 + y^2}$.) As shown in Figure 1, the interface between Ω_1 and Ω_2 is given by the curve Γ_0 and the boundaries of R_1 and R_2 are respectively the surfaces of revolution generated by rotating $\Gamma_0 \cup \Gamma_1$ and $\Gamma_0 \cup \Gamma_2$ about the z-axis, where Γ_1 and Γ_2 are curves which form outer boundaries of Ω_1 and Ω_2 respectively. In Figure 1, Γ_0, Γ_1 and Γ_2 are sketched as open curves, each with an endpoint on the z-axis. In general, they do not have to be always open curves with endpoints on the z-axis. For example, Γ_0 may be a horizontal straight line segment above the z-axis, that is, Γ_0 may be parallel to the z-axis. Furthermore, unlike in Figure 1, $\Gamma_1 \cup \Gamma_2$ may possibly form a simple closed curve as in, for example, the case in which $R_1 \cup R_2$ is a hollow cylinder.

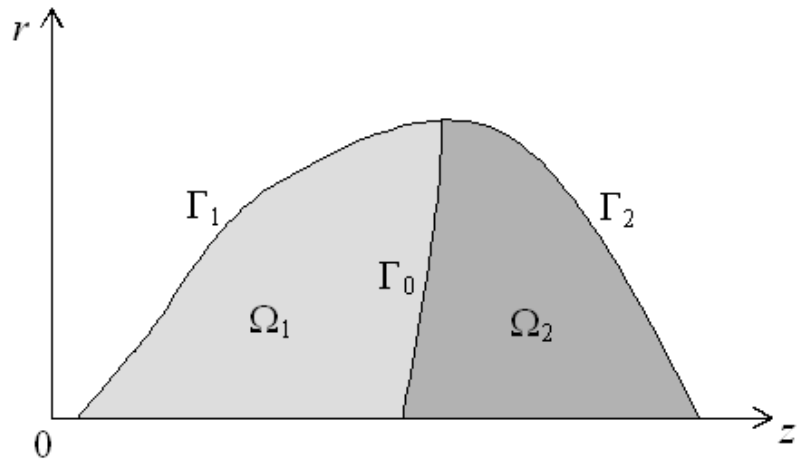

Figure 1. A geometrical sketch of the bimaterial on the rz plane.

The problem of interest here is to determine the steady-state axisymmetric temperature distribution $T(\underline{\mathbf{x}})$ by solving the governing partial differential equation

$$\frac{\partial^2 T}{\partial r^2} + \frac{1}{r}\frac{\partial T}{\partial r} + \frac{\partial^2 T}{\partial z^2} = 0 \quad \text{for } \underline{\mathbf{x}} = (r, z) \in \ \Omega_1 \cup \Omega_2, \tag{1}$$

subject to the boundary conditions

$$\begin{aligned} T(\underline{\mathbf{x}}) &= f_0(\underline{\mathbf{x}}) \text{ for } \underline{\mathbf{x}} \in \Xi_1, \\ P(\underline{\mathbf{x}}; \underline{\mathbf{n}}(\underline{\mathbf{x}})) &= f_1(\underline{\mathbf{x}}) + f_2(\underline{\mathbf{x}}) T(\underline{\mathbf{x}}) \text{ for } \underline{\mathbf{x}} \in \Xi_2, \end{aligned} \tag{2}$$

and the interfacial conditions given by either

$$\kappa_1 \, Q_1(\underline{\mathbf{x}}) \ = \kappa_2 \ Q_2(\underline{\mathbf{x}}) = \lambda(\underline{\mathbf{x}}) \Delta T(\underline{\mathbf{x}}) \text{ for } \underline{\mathbf{x}} \in \Gamma_0, \tag{3}$$

or

$$\left.\begin{aligned} \Delta T(\underline{\mathbf{x}}) = 0 \\ \kappa_1 \, Q_1(\underline{\mathbf{x}}) - \kappa_2 \ Q_2(\underline{\mathbf{x}}) = -\alpha(\underline{\mathbf{x}}) \mathcal{S}(T(\underline{\mathbf{x}})) \end{aligned}\right\} \text{ for } \underline{\mathbf{x}} \in \Gamma_0, \tag{4}$$

where $P(\underline{\mathbf{x}};\underline{\mathbf{n}}(\underline{\mathbf{x}})) = \underline{\mathbf{n}}(\underline{\mathbf{x}}) \bullet [\underline{\mathbf{e}}_r \partial T/\partial r + \underline{\mathbf{e}}_z \partial T/\partial z]$, $\underline{\mathbf{n}}(\underline{\mathbf{x}}) = [n_r(\underline{\mathbf{x}}), n_z(\underline{\mathbf{x}})] = n_r(\underline{\mathbf{x}})\underline{\mathbf{e}}_r + n_z(\underline{\mathbf{x}})\underline{\mathbf{e}}_z$, $\underline{\mathbf{e}}_r$ and $\underline{\mathbf{e}}_z$ are the unit base vectors along the r and z axes respectively, $f_0(\underline{\mathbf{x}})$, $f_1(\underline{\mathbf{x}})$ and $f_2(\underline{\mathbf{x}})$ are suitably prescribed functions, Ξ_1 and Ξ_2 are non-intersecting curves (for the different boundary conditions) such that $\Xi_1 \cup \Xi_2 = \Gamma_1 \cup \Gamma_2$, $\underline{\mathbf{n}}(\underline{\mathbf{x}})$ is the unit normal vector to $\Xi_1 \cup \Xi_2$ (at the point $\underline{\mathbf{x}}$) pointing out of $\Omega_1 \cup \Omega_2$, $\underline{\mathbf{n}}^{\text{int}}(\underline{\mathbf{x}})$ is the unit normal vector to Γ_0 (at $\underline{\mathbf{x}}$) pointing into Ω_1, $\underline{\mathbf{t}}^{\text{int}}(\underline{\mathbf{x}}) = [t_r^{\text{int}}(\underline{\mathbf{x}}), t_z^{\text{int}}(\underline{\mathbf{x}})]$ is a unit tangential vector to Γ_0 (at $\underline{\mathbf{x}}$), $\lambda(\underline{\mathbf{x}})$ and $\alpha(\underline{\mathbf{x}})$ are given positive functions, $Q_i(\underline{\mathbf{x}})$ (for $\underline{\mathbf{x}} \in \Gamma_0$) is the function $P(\underline{\mathbf{x}};\underline{\mathbf{n}}^{\text{int}}(\underline{\mathbf{x}}))$ calculated using the temperature field $T(\underline{\mathbf{x}})$ in Ω_i, $\Delta T(\underline{\mathbf{x}})$ is the temperature jump across Γ_0 (at $\underline{\mathbf{x}}$) as defined by

$$\Delta T(\underline{\mathbf{x}}) = \lim_{\varepsilon \to 0^+} [T(\underline{\mathbf{x}} + \varepsilon \underline{\mathbf{n}}^{\text{int}}(\underline{\mathbf{x}})) - T(\underline{\mathbf{x}} - \varepsilon \underline{\mathbf{n}}^{\text{int}}(\underline{\mathbf{x}}))] \text{ for } \underline{\mathbf{x}} \in \Gamma_0, \tag{5}$$

and $\mathcal{S}$ is the differential operator defined by

$$\mathcal{S} \equiv (t_r^{\text{int}}(\underline{\mathbf{x}})\frac{\partial}{\partial r} + t_z^{\text{int}}(\underline{\mathbf{x}})\frac{\partial}{\partial z})(t_r^{\text{int}}(\underline{\mathbf{x}})\frac{\partial}{\partial r} + t_z^{\text{int}}(\underline{\mathbf{x}})\frac{\partial}{\partial z}). \tag{6}$$

Note that (3) and (4) are the interfacial conditions on low conducting and high conducting interfaces respectively (Benveniste [4] and Miloh and Benveniste [8]).

3 Boundary integral equations in axisymmetric coordinates

For the problem under consideration here, the boundary integral equations for (1) (Brebbia, Telles and Wrobel [6]) give rise to

$$\begin{aligned}\gamma_1(\underline{\mathbf{x}}_0)T(\underline{\mathbf{x}}_0) = &\int_{\Gamma_1} (T(\underline{\mathbf{x}})G_1(\underline{\mathbf{x}};\underline{\mathbf{x}}_0;\underline{\mathbf{n}}(\underline{\mathbf{x}})) - G_0(\underline{\mathbf{x}};\underline{\mathbf{x}}_0)P(\underline{\mathbf{x}};\underline{\mathbf{n}}(\underline{\mathbf{x}})))rds(\underline{\mathbf{x}}) \\ &- \int_{\Gamma_0} (T(\underline{\mathbf{x}})G_1(\underline{\mathbf{x}};\underline{\mathbf{x}}_0;\underline{\mathbf{n}}^{\text{int}}(\underline{\mathbf{x}})) - G_0(\underline{\mathbf{x}};\underline{\mathbf{x}}_0)Q_1(\underline{\mathbf{x}}))rds(\underline{\mathbf{x}}) \\ &\text{for } \underline{\mathbf{x}}_0 = (r_0, z_0) \in \Omega_1 \cup \Gamma_0 \cup \Gamma_1, \end{aligned} \tag{7}$$

and

$$\gamma_2(\underline{\mathbf{x}}_0)T(\underline{\mathbf{x}}_0) = \int_{\Gamma_2} (T(\underline{\mathbf{x}})G_1(\underline{\mathbf{x}};\underline{\mathbf{x}}_0;\underline{\mathbf{n}}(\underline{\mathbf{x}})) - G_0(\underline{\mathbf{x}};\underline{\mathbf{x}}_0)P(\underline{\mathbf{x}};\underline{\mathbf{n}}(\underline{\mathbf{x}})))rds(\underline{\mathbf{x}})$$
$$+ \int_{\Gamma_0} (T(\underline{\mathbf{x}})G_1(\underline{\mathbf{x}};\underline{\mathbf{x}}_0;\underline{\mathbf{n}}^{\text{int}}(\underline{\mathbf{x}})) - G_0(\underline{\mathbf{x}};\underline{\mathbf{x}}_0)Q_2(\underline{\mathbf{x}}))rds(\underline{\mathbf{x}})$$
$$\text{for } \underline{\mathbf{x}}_0 = (r_0, z_0) \in \Omega_2 \cup \Gamma_0 \cup \Gamma_2, \quad (8)$$

where $\gamma_i(\underline{\mathbf{x}}_0) = 1$ if $\underline{\mathbf{x}}_0$ lies in the interior of Ω_i, $\gamma_i(\underline{\mathbf{x}}_0) = 1/2$ if $\underline{\mathbf{x}}_0$ lies on a smooth part of $\Gamma_0 \cup \Gamma_i$, $ds(\underline{\mathbf{x}})$ denotes the length of an infinitesimal part of the curve $\Gamma_0 \cup \Gamma_i$, $G_0(\underline{\mathbf{x}};\underline{\mathbf{x}}_0)$ and $G_1(\underline{\mathbf{x}};\underline{\mathbf{x}}_0;\underline{\mathbf{n}}(\underline{\mathbf{x}}))$ are defined by

$$G_0(\underline{\mathbf{x}};\underline{\mathbf{x}}_0) = -\frac{K(m(\underline{\mathbf{x}};\underline{\mathbf{x}}_0))}{\pi\sqrt{a(\underline{\mathbf{x}};\underline{\mathbf{x}}_0) + b(r;r_0)}},$$
$$G_1(\underline{\mathbf{x}};\underline{\mathbf{x}}_0;\underline{\mathbf{n}}(\underline{\mathbf{x}})) = -\frac{1}{\pi\sqrt{a(\underline{\mathbf{x}};\underline{\mathbf{x}}_0) + b(r;r_0)}}$$
$$\times \{\frac{n_r(\underline{\mathbf{x}})}{2r}[\frac{r_0^2 - r^2 + (z_0 - z)^2}{a(\underline{\mathbf{x}};\underline{\mathbf{x}}_0) - b(r;r_0)}E(m(\underline{\mathbf{x}};\underline{\mathbf{x}}_0))$$
$$- K(m(\underline{\mathbf{x}};\underline{\mathbf{x}}_0))]$$
$$+ n_z(\underline{\mathbf{x}})\frac{z_0 - z}{a(\underline{\mathbf{x}};\underline{\mathbf{x}}_0) - b(r;r_0)}E(m(\underline{\mathbf{x}};\underline{\mathbf{x}}_0))\}, \quad (9)$$

with

$$m(\underline{\mathbf{x}};\underline{\mathbf{x}}_0) = \frac{2b(r;r_0)}{a(\underline{\mathbf{x}};\underline{\mathbf{x}}_0) + b(r;r_0)},$$
$$a(\underline{\mathbf{x}};\underline{\mathbf{x}}_0) = r_0^2 + r^2 + (z_0 - z)^2, \quad b(r;r_0) = 2rr_0,$$
$$K(m) = \int_0^{\pi/2} \frac{d\theta}{\sqrt{1 - m\sin^2\theta}}, \quad E(m) = \int_0^{\pi/2} \sqrt{1 - m\sin^2\theta}\, d\theta. \quad (10)$$

Note again that $\underline{\mathbf{x}} = (r, z)$ and $\underline{\mathbf{x}}_0 = (r_0, z_0)$. Also, $K(m)$ and $E(m)$ are the complete elliptic integrals of the first and second kind respectively. The boundary integrals in (7) and (8) are improper and are to be interpreted in the Cauchy principal sense if $\underline{\mathbf{x}}_0$ lies on Γ_0 or Γ_1 or Γ_2.

4 Low conducting interfaces

4.1 Integral equations

For low conducting interfaces, addition of (7) and (8) together with the use of (3) yields

$$\gamma(\underline{\mathbf{x}}_0)T(\underline{\mathbf{x}}_0) = \int\limits_{\Gamma_1\cup\Gamma_2} [T(\underline{\mathbf{x}})G_1(\underline{\mathbf{x}};\underline{\mathbf{x}}_0;\underline{\mathbf{n}}(\underline{\mathbf{x}})) - G_0(\underline{\mathbf{x}};\underline{\mathbf{x}}_0)P(\underline{\mathbf{x}};\underline{\mathbf{n}}(\underline{\mathbf{x}}))]rds(\underline{\mathbf{x}})$$
$$- \int\limits_{\Gamma_0} \Delta T(\underline{\mathbf{x}})[G_1(\underline{\mathbf{x}};\underline{\mathbf{x}}_0;\underline{\mathbf{n}}^{\rm int}(\underline{\mathbf{x}})) - \frac{(\kappa_2-\kappa_1)}{\kappa_1\kappa_2}\lambda(\underline{\mathbf{x}})G_0(\underline{\mathbf{x}};\underline{\mathbf{x}}_0)]rds(\underline{\mathbf{x}})$$
$$\text{for } \underline{\mathbf{x}}_0 \in \Omega_1\cup\Omega_2\cup\Gamma_1\cup\Gamma_2, \qquad (11)$$

where $\gamma(\underline{\mathbf{x}}_0) = 1$ if $\underline{\mathbf{x}}_0$ lies in the interior of $\Omega_1\cup\Omega_2$ or on Γ_0 and $\gamma(\underline{\mathbf{x}}_0) = 1/2$ if $\underline{\mathbf{x}}_0$ lies on a smooth part of $\Gamma_1\cup\Gamma_2$.

From (11), we may write

$$n_r^{\rm int}(\underline{\mathbf{y}})\frac{\partial}{\partial r_0}[T(\underline{\mathbf{x}}_0)] + n_z^{\rm int}(\underline{\mathbf{y}})\frac{\partial}{\partial z_0}[T(\underline{\mathbf{x}}_0)]$$
$$= \int\limits_{\Gamma_1\cup\Gamma_2} [T(\underline{\mathbf{x}})\Phi_1(\underline{\mathbf{x}};\underline{\mathbf{x}}_0;\underline{\mathbf{n}}(\underline{\mathbf{x}});\underline{\mathbf{n}}^{\rm int}(\underline{\mathbf{y}}))$$
$$-\Phi_0(\underline{\mathbf{x}};\underline{\mathbf{x}}_0;\underline{\mathbf{n}}^{\rm int}(\underline{\mathbf{y}}))P(\underline{\mathbf{x}};\underline{\mathbf{n}}(\underline{\mathbf{x}}))]rds(\underline{\mathbf{x}})$$
$$- \int\limits_{\Gamma_0} \Delta T(\underline{\mathbf{x}})[\Phi_1(\underline{\mathbf{x}};\underline{\mathbf{x}}_0;\underline{\mathbf{n}}^{\rm int}(\underline{\mathbf{x}});\underline{\mathbf{n}}^{\rm int}(\underline{\mathbf{y}}))$$
$$-\frac{(\kappa_2-\kappa_1)}{\kappa_1\kappa_2}\lambda(\underline{\mathbf{x}})\Phi_0(\underline{\mathbf{x}};\underline{\mathbf{x}}_0;\underline{\mathbf{n}}^{\rm int}(\underline{\mathbf{y}}))]rds(\underline{\mathbf{x}})$$
$$\text{for } \underline{\mathbf{x}}_0 \text{ in the interior of } \Omega_1 \text{ or } \Omega_2, \qquad (12)$$

where $\underline{\mathbf{y}}$ is a point on the interface Γ_0 and the functions $\Phi_0(\underline{\mathbf{x}};\underline{\mathbf{x}}_0;\underline{\mathbf{n}}^{\rm int}(\underline{\mathbf{y}}))$ and $\Phi_1(\underline{\mathbf{x}};\underline{\mathbf{x}}_0;\underline{\mathbf{n}}(\underline{\mathbf{x}});\underline{\mathbf{n}}^{\rm int}(\underline{\mathbf{y}}))$ are given by

$$\Phi_0(\underline{\mathbf{x}};\underline{\mathbf{x}}_0;\underline{\mathbf{n}}^{\rm int}(\underline{\mathbf{y}})) = G_1(\underline{\mathbf{x}}_0;\underline{\mathbf{x}};\underline{\mathbf{n}}^{\rm int}(\underline{\mathbf{y}})),$$

$$\Phi_1(\underline{\mathbf{x}};\underline{\mathbf{x}}_0;\underline{\mathbf{n}}(\underline{\mathbf{x}});\underline{\mathbf{n}}^{\rm int}(\underline{\mathbf{y}}))$$
$$= \frac{n_r^{\rm int}(\underline{\mathbf{y}})\Theta(\underline{\mathbf{x}};\underline{\mathbf{x}}_0;\underline{\mathbf{n}}(\underline{\mathbf{x}})) + n_z^{\rm int}(\underline{\mathbf{y}})\Psi(\underline{\mathbf{x}};\underline{\mathbf{x}}_0;\underline{\mathbf{n}}(\underline{\mathbf{x}}))}{\pi\sqrt{a(\underline{\mathbf{x}};\underline{\mathbf{x}}_0)+b(r;r_0)}(a(\underline{\mathbf{x}};\underline{\mathbf{x}}_0)-b(r;r_0))^2}, \qquad (13)$$

with

$$
\begin{aligned}
\Theta(\underline{\mathbf{x}};\underline{\mathbf{x}}_0;\underline{\mathbf{n}}(\underline{\mathbf{x}})) &= (r+r_0)(1-m(\underline{\mathbf{x}};\underline{\mathbf{x}}_0))\{\frac{n_r(\underline{\mathbf{x}})}{2r} \\
&\times[\left(a(\underline{\mathbf{x}};\underline{\mathbf{x}}_0)-2r^2\right)E(m(\underline{\mathbf{x}};\underline{\mathbf{x}}_0)) \\
&-(a(\underline{\mathbf{x}};\underline{\mathbf{x}}_0)-b(r;r_0))K(m(\underline{\mathbf{x}};\underline{\mathbf{x}}_0))] \\
&-n_z(\underline{\mathbf{x}})(z-z_0)E(m(\underline{\mathbf{x}};\underline{\mathbf{x}}_0))\} \\
&-\frac{n_r(\underline{\mathbf{x}})}{2r_0}[\left(a(\underline{\mathbf{x}};\underline{\mathbf{x}}_0)-2r_0^2\right)(1-m(\underline{\mathbf{x}};\underline{\mathbf{x}}_0)) \\
&\times[(r-r_0)K(m(\underline{\mathbf{x}};\underline{\mathbf{x}}_0))-(r+r_0)E(m(\underline{\mathbf{x}};\underline{\mathbf{x}}_0))] \\
&-2r_0\left((r-r_0)^2-(z-z_0)^2\right)E(m(\underline{\mathbf{x}};\underline{\mathbf{x}}_0))] \\
&+\frac{n_z(\underline{\mathbf{x}})}{2r_0}(z-z_0)[4r_0(r-r_0)E(m(\underline{\mathbf{x}};\underline{\mathbf{x}}_0)) \\
&+(1-m(\underline{\mathbf{x}};\underline{\mathbf{x}}_0))\left(a(\underline{\mathbf{x}};\underline{\mathbf{x}}_0)-2r_0^2\right) \\
&\times\left(E(m(\underline{\mathbf{x}};\underline{\mathbf{x}}_0))-K(m(\underline{\mathbf{x}};\underline{\mathbf{x}}_0))\right)], \\
\Psi(\underline{\mathbf{x}};\underline{\mathbf{x}}_0;\underline{\mathbf{n}}(\underline{\mathbf{x}})) &= -\{(z-z_0)\left(1-m(\underline{\mathbf{x}};\underline{\mathbf{x}}_0)\right) \\
&\times[\frac{n_r(\underline{\mathbf{x}})}{2r}[\left(a(\underline{\mathbf{x}};\underline{\mathbf{x}}_0)-2r^2\right)E(m(\underline{\mathbf{x}};\underline{\mathbf{x}}_0)) \\
&-(a(\underline{\mathbf{x}};\underline{\mathbf{x}}_0)-b(r;r_0))K(m(\underline{\mathbf{x}};\underline{\mathbf{x}}_0))] \\
&-n_z(\underline{\mathbf{x}})(z-z_0)E(m(\underline{\mathbf{x}};\underline{\mathbf{x}}_0))] \\
&+n_r(\underline{\mathbf{x}})(z-z_0)[(1-m(\underline{\mathbf{x}};\underline{\mathbf{x}}_0)) \\
&\times[(r-r_0)K(m(\underline{\mathbf{x}};\underline{\mathbf{x}}_0))-(r+r_0)E(m(\underline{\mathbf{x}};\underline{\mathbf{x}}_0))] \\
&-2(r-r_0)E(m(\underline{\mathbf{x}};\underline{\mathbf{x}}_0))] \\
&-n_z(\underline{\mathbf{x}})[\left((2-m(\underline{\mathbf{x}};\underline{\mathbf{x}}_0))\,(z-z_0)^2\right. \\
&\left.-(r-r_0)^2\right)E(m(\underline{\mathbf{x}};\underline{\mathbf{x}}_0)) \\
&-(1-m(\underline{\mathbf{x}};\underline{\mathbf{x}}_0))\,(z-z_0)^2\,K(m(\underline{\mathbf{x}};\underline{\mathbf{x}}_0))]\}. \qquad (14)
\end{aligned}
$$

Noting that $K(m)$ can be expanded about $m=1$ as (see, for example, [9])

$$
\begin{aligned}
K(m) &= -\frac{1}{2}\ln(1-m)\cdot[1-\frac{1}{4}(m-1)+\frac{9}{64}(m-1)^2+\cdots] \\
&\quad +\ln(4)+\frac{1}{4}(1-\ln(4))(m-1)+\frac{3}{128}(6\ln(4)-7)(1-m)^2+\cdots, \qquad (15)
\end{aligned}
$$

and letting $\underline{\mathbf{x}}_0$ tend to $\underline{\mathbf{y}} = (\rho_0, \zeta_0)$ on Γ_0 (from within the region Ω_1), we find that the interfacial conditions in (3) give rise to

$$\begin{aligned}
&[\frac{1}{\kappa_1} - \frac{(\kappa_2 - \kappa_1)}{2\kappa_1\kappa_2}]\lambda(\underline{\mathbf{y}})\Delta T(\underline{\mathbf{y}}) \\
= \;& \mathcal{H}\int\limits_{\Gamma_0} \frac{\Delta T(\underline{\mathbf{x}})}{\sqrt{a(\underline{\mathbf{x}};\underline{\mathbf{y}}) + b(r;\rho_0)}}\Phi_3(\underline{\mathbf{x}};\underline{\mathbf{y}};\underline{\mathbf{n}}^{\rm int}(\underline{\mathbf{x}});\underline{\mathbf{n}}^{\rm int}(\underline{\mathbf{y}}))rds(\underline{\mathbf{x}}) \\
& -\mathcal{C}\int\limits_{\Gamma_0} \Delta T(\underline{\mathbf{x}})[\Phi_2(\underline{\mathbf{x}};\underline{\mathbf{y}};\underline{\mathbf{n}}^{\rm int}(\underline{\mathbf{x}});\underline{\mathbf{n}}^{\rm int}(\underline{\mathbf{y}})) \\
& -\frac{(\kappa_2 - \kappa_1)}{\kappa_1\kappa_2}\lambda(\underline{\mathbf{x}})\Phi_0(\underline{\mathbf{x}};\underline{\mathbf{y}};\underline{\mathbf{n}}^{\rm int}(\underline{\mathbf{y}}))]rds(\underline{\mathbf{x}}) \\
& +\int\limits_{\Gamma_1\cup\Gamma_2} [T(\underline{\mathbf{x}})\Phi_1(\underline{\mathbf{x}};\underline{\mathbf{y}};\underline{\mathbf{n}}(\underline{\mathbf{x}});\underline{\mathbf{n}}^{\rm int}(\underline{\mathbf{y}})) \\
& -\Phi_0(\underline{\mathbf{x}};\underline{\mathbf{y}};\underline{\mathbf{n}}^{\rm int}(\underline{\mathbf{y}}))P(\underline{\mathbf{x}};\underline{\mathbf{n}}(\underline{\mathbf{x}}))]rds(\underline{\mathbf{x}}) \\
& \qquad\qquad \text{for } \underline{\mathbf{y}} = (\rho_0, \zeta_0) \in \Gamma_0 \text{ (smooth part)}, \qquad (16)
\end{aligned}$$

where $\mathcal{C}$ and $\mathcal{H}$ denotes that the integral over Γ_0 is to be interpreted in the Cauchy principal and the Hadamard finite-part sense respectively and

$$\begin{aligned}
\Phi_2(\underline{\mathbf{x}};\underline{\mathbf{y}};\underline{\mathbf{n}}^{\rm int}(\underline{\mathbf{x}});\underline{\mathbf{n}}^{\rm int}(\underline{\mathbf{y}})) \;=\; & \Phi_1(\underline{\mathbf{x}};\underline{\mathbf{y}};\underline{\mathbf{n}}^{\rm int}(\underline{\mathbf{x}});\underline{\mathbf{n}}^{\rm int}(\underline{\mathbf{y}})) \\
& +\frac{\Phi_3(\underline{\mathbf{x}};\underline{\mathbf{y}};\underline{\mathbf{n}}^{\rm int}(\underline{\mathbf{x}});\underline{\mathbf{n}}^{\rm int}(\underline{\mathbf{y}}))}{\sqrt{a(\underline{\mathbf{x}};\underline{\mathbf{y}}) + b(r;\rho_0)}},
\end{aligned}$$

$$\begin{aligned}
& \Phi_3(\underline{\mathbf{x}};\underline{\mathbf{y}};\underline{\mathbf{n}}^{\rm int}(\underline{\mathbf{x}});\underline{\mathbf{n}}^{\rm int}(\underline{\mathbf{y}})) \\
= \;& -\{(n_r^{\rm int}(\underline{\mathbf{x}})n_r^{\rm int}(\underline{\mathbf{y}}) - n_z^{\rm int}(\underline{\mathbf{x}})n_z^{\rm int}(\underline{\mathbf{y}}))([r-\rho_0]^2 - [z-\zeta_0]^2) \\
& +2[n_r^{\rm int}(\underline{\mathbf{y}})n_z^{\rm int}(\underline{\mathbf{x}}) + n_r^{\rm int}(\underline{\mathbf{x}})n_z^{\rm int}(\underline{\mathbf{y}})] \\
& \times(r-\rho_0)(z-\zeta_0)\}\frac{1}{\pi(a(\underline{\mathbf{x}};\underline{\mathbf{y}}) - b(r;\rho_0))^2}.
\end{aligned} \qquad (17)$$

The derivation of (16) is given in Ang [1] for two-dimensional heat conduction across a low conducting interface. The fundamental solution of the governing partial differential equation for the two-dimensional heat conduction has a relatively simple form.

4.2 Boundary element procedure

If $T(\underline{\mathbf{x}})$ and $P(\underline{\mathbf{x}};\underline{\mathbf{n}}(\underline{\mathbf{x}}))$ are completely known on $\Gamma_1 \cup \Gamma_2$ and if the temperature jump $\Delta T(\underline{\mathbf{x}})$ across the weak conducting interface Γ_0 is also known, (11) together with $\gamma(\underline{\mathbf{x}}_0) = 1$ gives the temperature at any point $\underline{\mathbf{x}}_0$ in the interior of Ω_1 or Ω_2. Here we describe a boundary element procedure for determining $T(\underline{\mathbf{x}})$ or $P(\underline{\mathbf{x}};\underline{\mathbf{n}}(\underline{\mathbf{x}}))$ (whichever is unknown) on $\Gamma_1 \cup \Gamma_2$ and also $\Delta T(\underline{\mathbf{x}})$ on Γ_0.

We discretize the boundary $\Gamma_1 \cup \Gamma_2$ into N straight line elements denoted by $B^{(1)}$, $B^{(2)}$, $\cdots$, $B^{(N-1)}$ and $B^{(N)}$ and the interface Γ_0 into M elements $I^{(1)}$, $I^{(2)}$, $\cdots$, $I^{(M-1)}$ and $I^{(M)}$. For a simple approximation, over an element of $\Gamma_1 \cup \Gamma_2$, T and P are taken to be constants. Also, over an element of the interface, ΔT is approximated as a constant. Specifically, we make the approximation:

$$\left.\begin{array}{c} T(\underline{\mathbf{x}}) \simeq T^{(k)} \\ P(\underline{\mathbf{x}};\underline{\mathbf{n}}(\underline{\mathbf{x}})) \simeq P^{(k)} \end{array}\right\} \quad \text{for } \underline{\mathbf{x}} \in B^{(k)} \ (k = 1, 2, \cdots, N),$$

$$\Delta T(\underline{\mathbf{x}}) \simeq \Delta T^{(j)} \quad \text{for } \underline{\mathbf{x}} \in I^{(j)} \ (j = 1, 2, \cdots, M), \tag{18}$$

where $T^{(k)}$, $P^{(k)}$ and $\Delta T^{(j)}$ are constants.

If we let $\underline{\mathbf{x}}_0$ in (11) be given in turn by each of the midpoints of $B^{(1)}$, $B^{(2)}$, $\cdots$, $B^{(N-1)}$ and $B^{(N)}$, the use of (2) and (18) approximately gives

$$\begin{aligned}
&\frac{1}{2}[d^{(i)}T^{(i)} + (1-d^{(i)})f_0(\widehat{\underline{\mathbf{x}}}^{(i)})] \\
= &\sum_{k=1}^{N}\{[d^{(k)}T^{(k)} + (1-d^{(k)})f_0(\widehat{\underline{\mathbf{x}}}^{(k)})] \int\limits_{B^{(k)}} G_1(\underline{\mathbf{x}};\widehat{\underline{\mathbf{x}}}^{(i)};\underline{\mathbf{n}}^{(k)})rds(\underline{\mathbf{x}}) \\
&-[d^{(k)}(f_1(\widehat{\underline{\mathbf{x}}}^{(k)}) + f_2(\widehat{\underline{\mathbf{x}}}^{(k)})T^{(k)}) + (1-d^{(k)})P^{(k)}] \\
&\times \int\limits_{B^{(k)}} G_0(\underline{\mathbf{x}};\widehat{\underline{\mathbf{x}}}^{(i)})rds(\underline{\mathbf{x}})\} \\
&-\sum_{j=1}^{M} \Delta T^{(j)} \int\limits_{I^{(j)}} [G_1(\underline{\mathbf{x}};\widehat{\underline{\mathbf{x}}}^{(i)};\underline{\mathbf{m}}^{(j)}) - \frac{(\kappa_2-\kappa_1)}{\kappa_1\kappa_2}\lambda(\underline{\mathbf{x}})G_0(\underline{\mathbf{x}};\widehat{\underline{\mathbf{x}}}^{(i)})]rds(\underline{\mathbf{x}}) \\
&\qquad\qquad \text{for } i = 1,\ 2, \cdots, N.
\end{aligned} \tag{19}$$

where $d^{(k)} = 0$ if T is specified on the k-th element $B^{(k)}$ as given by the first line of (2), $d^{(k)} = 1$ if the boundary condition given by the second line of (2) is applicable on $B^{(k)}$, $\underline{\mathbf{n}}^{(k)}$ is the unit normal vector to $B^{(k)}$ pointing away from the solution domain $\Omega_1 \cup \Omega_2$, $\underline{\mathbf{m}}^{(j)}$ is the unit normal vector to $I^{(j)}$ pointing into Ω_1 and $\widehat{\underline{\mathbf{x}}}^{(i)}$ is the midpoint of the element $B^{(i)}$. In (19), note that the integrals over $B^{(k)}$ are Cauchy principal if $\widehat{\underline{\mathbf{x}}}^{(i)}$ is the midpoint of $B^{(k)}$ (that is, if $k = i$). The Cauchy principal integrals can be accurately evaluated by using a highly accurate Gaussian quadrature.

Similarly, we can let $\underline{\mathbf{y}}$ in (16) be given in turn by each of the midpoints of $I^{(1)}$, $I^{(2)}$, $\cdots$, $I^{(M-1)}$ and $I^{(M)}$ to approximately obtain

$$
\begin{aligned}
& [(\frac{1}{\kappa_1} - \frac{(\kappa_2 - \kappa_1)}{2\kappa_1\kappa_2})\lambda(\widehat{\underline{\mathbf{y}}}^{(p)}) + \frac{2}{\pi\ell^{(p)}}]\Delta T^{(p)} \\
= & \sum_{\substack{j=1 \\ j\neq p}}^{M} \Delta T^{(j)} \int\limits_{I^{(j)}} \frac{\Phi_3(\underline{\mathbf{x}}; \widehat{\underline{\mathbf{y}}}^{(p)}; \underline{\mathbf{m}}^{(j)}; \underline{\mathbf{m}}^{(p)})}{\sqrt{a(\underline{\mathbf{x}}; \widehat{\underline{\mathbf{y}}}^{(p)}) + b(r; \widehat{\rho}_0^{(p)})}} r ds(\underline{\mathbf{x}}) \\
& - \sum_{j=1}^{M} \Delta T^{(j)} \int\limits_{I^{(j)}} [\Phi_2(\underline{\mathbf{x}}; \widehat{\underline{\mathbf{y}}}^{(p)}; \underline{\mathbf{m}}^{(j)}; \underline{\mathbf{m}}^{(p)}) \\
& - \frac{(\kappa_2 - \kappa_1)}{\kappa_1\kappa_2}\lambda(\underline{\mathbf{x}})\Phi_0(\underline{\mathbf{x}}; \widehat{\underline{\mathbf{y}}}^{(p)}; \underline{\mathbf{m}}^{(p)})] r ds(\underline{\mathbf{x}}) \\
& + \sum_{k=1}^{N} \{[d^{(k)}T^{(k)} + (1 - d^{(k)}) f_0(\widehat{\underline{\mathbf{x}}}^{(k)})] \int\limits_{B^{(k)}} \Phi_1(\underline{\mathbf{x}}; \widehat{\underline{\mathbf{y}}}^{(p)}; \underline{\mathbf{n}}^{(k)}; \underline{\mathbf{m}}^{(p)}) r ds(\underline{\mathbf{x}}) \\
& - [d^{(k)}(f_1(\widehat{\underline{\mathbf{x}}}^{(k)}) + f_2(\widehat{\underline{\mathbf{x}}}^{(k)})T^{(k)}) + (1 - d^{(k)})P^{(k)}] \\
& \times \int\limits_{B^{(k)}} \Phi_0(\underline{\mathbf{x}}; \widehat{\underline{\mathbf{y}}}^{(p)}; \underline{\mathbf{m}}^{(p)}) r ds(\underline{\mathbf{x}})\} \\
& \qquad\qquad \text{for } p = 1, 2, \cdots, M, \qquad (20)
\end{aligned}
$$

where $\ell^{(p)}$ and $\widehat{\underline{\mathbf{y}}}^{(p)} = (\widehat{\rho}_0^{(p)}, \widehat{\zeta}_0^{(p)})$ are respectively the length and the midpoint of $I^{(p)}$.

Note that in deriving (20) the Hadamard finite-part integral in (16) is evaluated by using the approximation

$$\begin{aligned}
&\mathcal{H}\int_{\Gamma_0}\frac{\Delta T(\underline{\mathbf{x}})}{\sqrt{a(\underline{\mathbf{x}};\underline{\mathbf{y}})+b(r;\rho_0)}}\Phi_3(\underline{\mathbf{x}};\underline{\mathbf{y}}\,;\underline{\mathbf{n}}^{\rm int}(\underline{\mathbf{x}});\underline{\mathbf{n}}^{\rm int}(\underline{\mathbf{y}}))rds(\underline{\mathbf{x}})\\
\simeq\;&\Delta T^{(p)}\mathcal{H}\int_{I^{(p)}}\frac{\Phi_3(\underline{\mathbf{x}};\widehat{\underline{\mathbf{y}}}^{(p)}\,;\underline{\mathbf{m}}^{(p)};\underline{\mathbf{m}}^{(p)})}{\sqrt{a(\underline{\mathbf{x}};\widehat{\underline{\mathbf{y}}}^{(p)})+b(r;\widehat{\rho}_0^{(p)})}}rds(\underline{\mathbf{x}})\\
&+\sum_{\substack{j=1\\ j\neq p}}^{M}\Delta T^{(j)}\int_{I^{(j)}}\frac{\Phi_3(\underline{\mathbf{x}};\widehat{\underline{\mathbf{y}}}^{(p)}\,;\underline{\mathbf{m}}^{(j)};\underline{\mathbf{m}}^{(p)})}{\sqrt{a(\underline{\mathbf{x}};\widehat{\underline{\mathbf{y}}}^{(p)})+b(r;\widehat{\rho}_0^{(p)})}}rds(\underline{\mathbf{x}}).
\end{aligned}\tag{21}$$

From (17), if the expression $r/\sqrt{a(\underline{\mathbf{x}};\widehat{\underline{\mathbf{y}}}^{(p)})+b(r;\widehat{\rho}_0^{(p)})}$ is approximated as a constant given by its value at the midpoint of $I^{(p)}$, the Hadamard finite-part integral on the right hand side of (21) is approximately given by $-2/(\pi\ell^{(p)})$.

The integrals over $I^{(j)}$ in (20) which have the functions Φ_0 and Φ_2 in their integrands approximate the Cauchy principal integral in (16). Hence the integrals over $I^{(j)}$ must be interpreted in the Cauchy principal sense if $\widehat{\underline{\mathbf{y}}}^{(p)}$ is the midpoint of $I^{(j)}$ (that is, if $j=p$). The integrals over $I^{(j)}$ in (20) are proper if $j\neq p$. The integrals over $B^{(k)}$ are also proper.

The equations in (19) and (20) give a system of $N+M$ linear algebraic equations containing $N+M$ unknowns given by either $T^{(k)}$ or $P^{(k)}$ (not both) for $k=1,\,2,\,\cdots,\,N$ and by $\Delta T^{(j)}$ for $j=1,\,2,\,\cdots,\,M$. If T is specified over the element $B^{(k)}$ according to the first line of (2) then $P^{(k)}$ is an unknown. On the other hand, if P is given by the second line of (2) over $B^{(k)}$ then $T^{(k)}$ is unknown. Once the unknowns are determined, the temperature at any interior point $\underline{\mathbf{x}}_0$ in the bimaterial can be determined from (11) with $\gamma(\underline{\mathbf{x}}_0)=1$ by computing approximately the line integrals over Γ_0 and $\Gamma_1\cup\Gamma_2$.

5 High conducting interfaces

5.1 Integral equations

From (7) and (8) and the zero temperature jump across the interface in (4), we obtain

$$\begin{aligned}\gamma(\underline{\mathbf{x}}_0)T(\underline{\mathbf{x}}_0) &= \int\limits_{\Gamma_1\cup\Gamma_2} [T(\underline{\mathbf{x}})G_1(\underline{\mathbf{x}};\underline{\mathbf{x}}_0;\underline{\mathbf{n}}(\underline{\mathbf{x}})) - G_0(\underline{\mathbf{x}};\underline{\mathbf{x}}_0)P(\underline{\mathbf{x}};\underline{\mathbf{n}}(\underline{\mathbf{x}}))]rds(\underline{\mathbf{x}}) \\ &\quad + \int\limits_{\Gamma_0} G_0(\underline{\mathbf{x}};\underline{\mathbf{x}}_0)[Q_1(\underline{\mathbf{x}}) - Q_2(\underline{\mathbf{x}})]rds(\underline{\mathbf{x}}). \qquad (22)\end{aligned}$$

From (22), we may write

$$\begin{aligned}&n_r^{\text{int}}(\underline{\mathbf{y}})\frac{\partial}{\partial r_0}[T(\underline{\mathbf{x}}_0)] + n_z^{\text{int}}(\underline{\mathbf{y}})\frac{\partial}{\partial z_0}[T(\underline{\mathbf{x}}_0)] \\ &= \int\limits_{\Gamma_1\cup\Gamma_2} [T(\underline{\mathbf{x}})\Phi_1(\underline{\mathbf{x}};\underline{\mathbf{x}}_0;\underline{\mathbf{n}}(\underline{\mathbf{x}});\underline{\mathbf{n}}^{\text{int}}(\underline{\mathbf{y}})) \\ &\quad -\Phi_0(\underline{\mathbf{x}};\underline{\mathbf{x}}_0;\underline{\mathbf{n}}^{\text{int}}(\underline{\mathbf{y}}))P(\underline{\mathbf{x}};\underline{\mathbf{n}}(\underline{\mathbf{x}}))]rds(\underline{\mathbf{x}}) \\ &\quad + \int\limits_{\Gamma_0} \Phi_0(\underline{\mathbf{x}};\underline{\mathbf{x}}_0;\underline{\mathbf{n}}^{\text{int}}(\underline{\mathbf{y}}))[Q_1(\underline{\mathbf{x}}) - Q_2(\underline{\mathbf{x}})]rds(\underline{\mathbf{x}}) \\ &\qquad\qquad \text{for } \underline{\mathbf{x}}_0 \text{ in the interior of } \Omega_1 \text{ or } \Omega_2, \qquad (23)\end{aligned}$$

where $\underline{\mathbf{y}}$ is a point on the interface Γ_0.

If we let $\underline{\mathbf{x}}_0$ tends to the point $\underline{\mathbf{y}}$ on Γ_0 (from within the region Ω_1), we obtain

$$\begin{aligned}&\frac{1}{2}[Q_1(\underline{\mathbf{y}}) + Q_2(\underline{\mathbf{y}})] \\ &= \int\limits_{\Gamma_1\cup\Gamma_2} [T(\underline{\mathbf{x}})\Phi_1(\underline{\mathbf{x}};\underline{\mathbf{y}};\underline{\mathbf{n}}(\underline{\mathbf{x}});\underline{\mathbf{n}}^{\text{int}}(\underline{\mathbf{y}})) \\ &\quad -\Phi_0(\underline{\mathbf{x}};\underline{\mathbf{y}};\underline{\mathbf{n}}^{\text{int}}(\underline{\mathbf{y}}))P(\underline{\mathbf{x}};\underline{\mathbf{n}}(\underline{\mathbf{x}}))]rds(\underline{\mathbf{x}}) \\ &\quad +\mathcal{C}\int\limits_{\Gamma_0} \Phi_0(\underline{\mathbf{x}};\underline{\mathbf{y}};\underline{\mathbf{n}}^{\text{int}}(\underline{\mathbf{y}}))[Q_1(\underline{\mathbf{x}}) - Q_2(\underline{\mathbf{x}})]rds(\underline{\mathbf{x}}) \\ &\qquad \text{for } \underline{\mathbf{y}} \in \Gamma_0 \text{ (smooth part).} \qquad (24)\end{aligned}$$

5.2 Boundary element procedure

The exterior boundary $\Gamma_1 \cup \Gamma_2$ and the interface Γ_0 are discretized into elements as described in Section 4.2. In addition to approximating $T(\underline{\mathbf{x}})$ and $P(\underline{\mathbf{x}}; \underline{\mathbf{n}}(\underline{\mathbf{x}}))$ as constants $T^{(k)}$ and $P^{(k)}$ respectively, as in (18), we make the approximation

$$Q_i(\underline{\mathbf{x}}) \simeq Q_i^{(m)} \text{ for } \underline{\mathbf{x}} \in I^{(m)} \ (m = 1, 2, \cdots, M), \tag{25}$$

where $Q_i^{(m)}$ are constants.

From (22), we obtain

$$\begin{aligned} \gamma(\underline{\mathbf{x}}_0)T(\underline{\mathbf{x}}_0) &= \sum_{k=1}^{N} \{T^{(k)} \int_{B^{(k)}} G_1(\underline{\mathbf{x}}; \underline{\mathbf{x}}_0; \underline{\mathbf{n}}^{(k)}) r ds(\underline{\mathbf{x}}) \\ &\quad - P^{(k)} \int_{B^{(k)}} G_0(\underline{\mathbf{x}}; \underline{\mathbf{x}}_0) r ds(\underline{\mathbf{x}})\} \\ &\quad + \sum_{m=1}^{M} (Q_1^{(m)} - Q_2^{(m)}) \int_{I^{(m)}} G_0(\underline{\mathbf{x}}; \underline{\mathbf{x}}_0) r ds(\underline{\mathbf{x}}). \end{aligned} \tag{26}$$

Collocating (26) at the midpoint of each boundary element and using the boundary conditions in (2) give

$$\begin{aligned} & \frac{1}{2}[d^{(i)}T^{(i)} + (1 - d^{(i)}) f_0(\widehat{\underline{\mathbf{x}}}^{(i)})] \\ = & \sum_{k=1}^{N} \{[d^{(k)}T^{(k)} + (1 - d^{(k)}) f_0(\widehat{\underline{\mathbf{x}}}^{(k)})] \int_{B^{(k)}} G_1(\underline{\mathbf{x}}; \widehat{\underline{\mathbf{x}}}^{(i)}; \underline{\mathbf{n}}^{(k)}) r ds(\underline{\mathbf{x}}) \\ & - [d^{(k)}(f_1(\widehat{\underline{\mathbf{x}}}^{(k)}) + f_2(\widehat{\underline{\mathbf{x}}}^{(k)})T^{(k)}) + (1 - d^{(k)})P^{(k)}] \\ & \times \int_{B^{(k)}} G_0(\underline{\mathbf{x}}; \widehat{\underline{\mathbf{x}}}^{(i)}) r ds(\underline{\mathbf{x}})\} \\ & + \sum_{m=1}^{M} (Q_1^{(m)} - Q_2^{(m)}) \int_{I^{(m)}} G_0(\underline{\mathbf{x}}; \widehat{\underline{\mathbf{x}}}^{(i)}) r ds(\underline{\mathbf{x}}) \\ & \qquad \text{for } i = 1, \ 2, \cdots, N. \end{aligned} \tag{27}$$

Similarly, from (24), we obtain

$$\begin{aligned}
&\frac{1}{2}[Q_1^{(i)} + Q_2^{(i)}] \\
= &\sum_{k=1}^{N}\{[d^{(k)}T^{(k)} + (1-d^{(k)})f_0(\widehat{\underline{\mathbf{x}}}^{(k)})] \int\limits_{B^{(k)}} \Phi_1(\underline{\mathbf{x}}; \widehat{\underline{\mathbf{y}}}^{(i)}; \underline{\mathbf{n}}^{(k)}; \underline{\mathbf{m}}^{(i)}) r ds(\underline{\mathbf{x}}) \\
&-[d^{(k)}(f_1(\widehat{\underline{\mathbf{x}}}^{(k)}) + f_2(\widehat{\underline{\mathbf{x}}}^{(k)})T^{(k)}) + (1-d^{(k)})P^{(k)}] \\
&\times \int\limits_{B^{(k)}} \Phi_0(\underline{\mathbf{x}}; \widehat{\underline{\mathbf{y}}}^{(i)}; \underline{\mathbf{m}}^{(i)}) r ds(\underline{\mathbf{x}})\} \\
&+\sum_{m=1}^{M}(Q_1^{(m)} - Q_2^{(m)}) \int\limits_{I^{(m)}} \Phi_0(\underline{\mathbf{x}}; \widehat{\underline{\mathbf{y}}}^{(i)}; \underline{\mathbf{m}}^{(i)}) r ds(\underline{\mathbf{x}}) \\
&\qquad\qquad \text{for } i = 1,\ 2, \cdots, M. \qquad (28)
\end{aligned}$$

To deal with the interfacial condition over $I^{(i)}$, as given in the second line of (4), we work out a formula for $\mathcal{S}(T(\underline{\mathbf{x}}))$ at $\underline{\mathbf{x}} \in I^{(i)}$ as follows.

From (26), we find that

$$\begin{aligned}
&t_r^{(i)}\frac{\partial}{\partial r_0}(T(\underline{\mathbf{x}}_0)) + t_z^{(i)}\frac{\partial}{\partial z_0}(T(\underline{\mathbf{x}}_0)) \\
= &\sum_{k=1}^{N}\{T^{(k)} \int\limits_{B^{(k)}} \Phi_1(\underline{\mathbf{x}}; \underline{\mathbf{x}}_0; \underline{\mathbf{n}}^{(k)}; \underline{\mathbf{t}}^{(i)}) r ds(\underline{\mathbf{x}}) \\
&-P^{(k)} \int\limits_{B^{(k)}} \Phi_0(\underline{\mathbf{x}}; \underline{\mathbf{x}}_0; \underline{\mathbf{t}}^{(i)}) r ds(\underline{\mathbf{x}})\} \\
&+\sum_{m=1}^{M}(Q_1^{(m)} - Q_2^{(m)}) \int\limits_{I^{(m)}} \Phi_0(\underline{\mathbf{x}}; \underline{\mathbf{x}}_0; \underline{\mathbf{t}}^{(i)}) r ds(\underline{\mathbf{x}}) \\
&\qquad \text{for } \underline{\mathbf{x}}_0 \text{ in the interior of } \Omega_1 \text{ or } \Omega_2, \qquad (29)
\end{aligned}$$

where $\underline{\mathbf{t}}^{(i)} = [t_r^{(i)}, t_z^{(i)}]$ is a unit tangential vector to the i-th interface element $I^{(i)}$.

It follows that

$$\begin{aligned}\mathcal{S}(T(\underline{\mathbf{x}}))|_{\underline{\mathbf{x}}=\underline{\mathbf{x}}_0} &= \sum_{k=1}^{N}\{T^{(k)}\int\limits_{B^{(k)}}\Lambda_1(\underline{\mathbf{x}};\underline{\mathbf{x}}_0;\underline{\mathbf{n}}^{(k)};\underline{\mathbf{t}}^{(i)})rds(\underline{\mathbf{x}})\\ &\quad -P^{(k)}\int\limits_{B^{(k)}}\Lambda_0(\underline{\mathbf{x}};\underline{\mathbf{x}}_0;\underline{\mathbf{t}}^{(i)})rds(\underline{\mathbf{x}})\}\\ &\quad +\sum_{m=1}^{M}(Q_1^{(m)}-Q_2^{(m)})\int\limits_{I^{(m)}}\Lambda_0(\underline{\mathbf{x}};\underline{\mathbf{x}}_0;\underline{\mathbf{t}}^{(i)})rds(\underline{\mathbf{x}})\\ &\quad \text{for } \underline{\mathbf{x}}_0 \text{ in the interior of } \Omega_1 \text{ or } \Omega_2, \qquad (30)\end{aligned}$$

where

$$\begin{aligned}\Lambda_0(\underline{\mathbf{x}};\underline{\mathbf{x}}_0;\underline{\mathbf{t}}^{(i)}) &= t_r^{(i)}\frac{\partial}{\partial r_0}[\Phi_0(\underline{\mathbf{x}};\underline{\mathbf{x}}_0;\underline{\mathbf{t}}^{(i)})]+t_z^{(i)}\frac{\partial}{\partial z_0}[\Phi_0(\underline{\mathbf{x}};\underline{\mathbf{x}}_0;\underline{\mathbf{t}}^{(i)})],\\ \Lambda_1(\underline{\mathbf{x}};\underline{\mathbf{x}}_0;\underline{\mathbf{n}}^{(k)};\underline{\mathbf{t}}^{(i)}) &= t_r^{(i)}\frac{\partial}{\partial r_0}[\Phi_1(\underline{\mathbf{x}};\underline{\mathbf{x}}_0;\underline{\mathbf{n}}^{(k)};\underline{\mathbf{t}}^{(i)})]\\ &\quad +t_z^{(i)}\frac{\partial}{\partial z_0}[\Phi_1(\underline{\mathbf{x}};\underline{\mathbf{x}}_0;\underline{\mathbf{n}}^{(k)};\underline{\mathbf{t}}^{(i)})]. \qquad (31)\end{aligned}$$

Explicit expressions for the partial derivatives of Φ_0 and Φ_1 which are quite complicated are banished to the Appendix.

If we let $\underline{\mathbf{x}}_0$ in (30) be given by $\widehat{\underline{\mathbf{y}}}^{(i)}$ (midpoint of $I^{(i)}$), the integral over $I^{(m)}$ is proper if $i \neq m$. For $i = m$, the limit of the integral as $\underline{\mathbf{x}}_0$ approaches as $\widehat{\underline{\mathbf{y}}}^{(m)}$ can be written as the sum of a Hadamard finite-part integral and a Cauchy principal integral, that is,

$$\begin{aligned}\int\limits_{I^{(m)}}\Lambda_0(\underline{\mathbf{x}};\underline{\mathbf{x}}_0;\underline{\mathbf{t}}^{(m)})rds(\underline{\mathbf{x}}) &= \mathcal{H}\int\limits_{I^{(m)}}\frac{\Phi_3(\underline{\mathbf{x}};\widehat{\underline{\mathbf{y}}}^{(m)};\underline{\mathbf{t}}^{(m)};\underline{\mathbf{t}}^{(m)})}{\sqrt{a(\underline{\mathbf{x}};\widehat{\underline{\mathbf{y}}}^{(m)})+b(r;\widehat{\rho}_0^{(m)})}}rds(\underline{\mathbf{x}})\\ &\quad +\mathcal{C}\int\limits_{I^{(m)}}\Phi_4(\underline{\mathbf{x}};\widehat{\underline{\mathbf{y}}}^{(m)};\underline{\mathbf{t}}^{(m)};\underline{\mathbf{t}}^{(m)})rds(\underline{\mathbf{x}}), \qquad (32)\end{aligned}$$

where

$$\begin{aligned}&\Phi_4(\underline{\mathbf{x}};\widehat{\underline{\mathbf{y}}}^{(m)};\underline{\mathbf{t}}^{(m)};\underline{\mathbf{t}}^{(m)})\\ &= \Lambda_0(\underline{\mathbf{x}};\widehat{\underline{\mathbf{y}}}^{(m)};\underline{\mathbf{t}}^{(m)})-\frac{\Phi_3(\underline{\mathbf{x}};\widehat{\underline{\mathbf{y}}}^{(m)};\underline{\mathbf{t}}^{(m)};\underline{\mathbf{t}}^{(m)})}{\sqrt{a(\underline{\mathbf{x}};\widehat{\underline{\mathbf{y}}}^{(m)})+b(r;\widehat{\rho}_0^{(m)})}}. \qquad (33)\end{aligned}$$

The Hadamard finite-part integral above which contains the function Φ_3 in its integrand has also appeared in the boundary element formulation for the low conducting interface. As explained below (21), it is approximately given by $-2/(\pi\ell^{(m)})$.

Thus, the interfacial condition in the second line of (4) becomes

$$\begin{aligned}
&\kappa_1 Q_1^{(i)} - \kappa_2 Q_2^{(i)} \\
= \; & -\alpha(\underline{\widehat{\mathbf{y}}}^{(i)}) \sum_{k=1}^{N} \{[d^{(k)} T^{(k)} + (1-d^{(k)}) f_0(\underline{\widehat{\mathbf{x}}}^{(k)})] \\
& \times \int_{B^{(k)}} \Lambda_1(\underline{\mathbf{x}}; \underline{\widehat{\mathbf{y}}}^{(i)}; \underline{\mathbf{n}}^{(k)}; \underline{\mathbf{t}}^{(i)}) r ds(\underline{\mathbf{x}}) \\
& -[d^{(k)}(f_1(\underline{\widehat{\mathbf{x}}}^{(k)}) + f_2(\underline{\widehat{\mathbf{x}}}^{(k)}) T^{(k)}) + (1-d^{(k)}) P^{(k)}] \\
& \times \int_{B^{(k)}} \Lambda_0(\underline{\mathbf{x}}; \underline{\widehat{\mathbf{y}}}^{(i)}; \underline{\mathbf{t}}^{(i)}) r ds(\underline{\mathbf{x}})\} - \alpha(\underline{\widehat{\mathbf{y}}}^{(i)}) \sum_{m=1}^{M} (Q_1^{(m)} - Q_2^{(m)}) L^{(im)} \\
& \qquad \text{for } i = 1, 2, \cdots, M,
\end{aligned} \tag{34}$$

where

$$\begin{aligned}
L^{(im)} &= \int_{I^{(m)}} \Lambda_0(\underline{\mathbf{x}}; \underline{\widehat{\mathbf{y}}}^{(i)}; \underline{\mathbf{t}}^{(i)}) r ds(\underline{\mathbf{x}}) \text{ for } i \neq m, \\
L^{(mm)} &\simeq \frac{2}{\pi\ell^{(m)}} + \mathcal{C} \int_{I^{(m)}} \Phi_4(\underline{\mathbf{x}}; \underline{\widehat{\mathbf{y}}}^{(m)}; \underline{\mathbf{t}}^{(m)}; \underline{\mathbf{t}}^{(m)})) r ds(\underline{\mathbf{x}}).
\end{aligned} \tag{35}$$

Equations (27), (28) and (34) can be solved as a system of $N+2M$ linear algebraic equations for $N+2M$ unknowns given by either $T^{(k)}$ or $P^{(k)}$ ($k = 1$, $2, \cdots, N$) and $Q_i^{(m)}$ ($i = 1, 2$ and $m = 1, 2, \cdots, M$).

6 Specific problems

Problem 1. To test the boundary element procedure for low conducting interfaces, take

$$\begin{aligned}
\Omega_1 &= \{(r,z) : \; r_{\text{int}} < r < r_{\text{outer}}, \; 0 < z < h\}, \\
\Omega_2 &= \{(r,z) : \; r_{\text{inner}} < r < r_{\text{int}}, \; 0 < z < h\},
\end{aligned}$$

where $r_{\rm int}$, $r_{\rm inner}$ and $r_{\rm outer}$ are constants such that $0 < r_{\rm inner} < r_{\rm int} < r_{\rm outer}$ and h is a given positive constant. Note that the weak conducting interface Γ_0 between Ω_1 and Ω_2 lies in the region $r = r_{\rm int}$, $0 < z < h$. Refer to Figure 2.

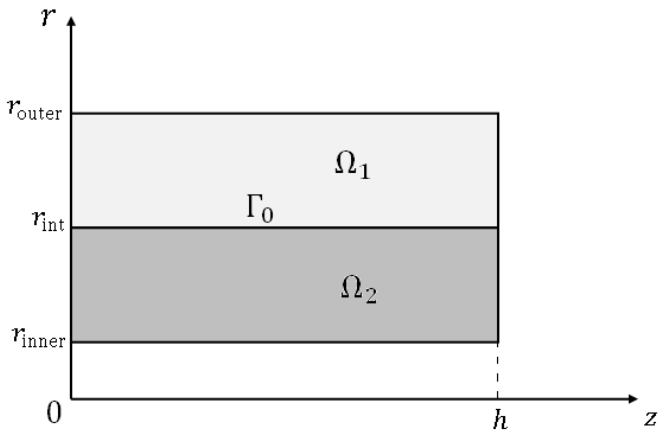

Figure 2. A geometrical sketch of Problem 1 on the rz plane.

The boundary conditions on the exterior boundary of $\Omega_1 \cup \Omega_2$ are given by

$$\begin{aligned} T(r_{\rm inner}, z) &= T_{\rm c} \text{ for } 0 < z < h, \\ P(r_{\rm outer}, z; 1, 0) &= -\frac{c}{\kappa_1}(T(r_{\rm outer}, z) - T_{\rm a}) \text{ for } 0 < z < h, \\ P(r, 0; 0, -1) &= P(r, h; 0, 1) = 0 \text{ for } r_{\rm inner} < r < r_{\rm outer}, \end{aligned}$$

where c, $T_{\rm c}$ and $T_{\rm a}$ are given constants. Note that $T_{\rm a}$ is the outside ambient temperature surrounding the body.

It is assumed that (3) is applicable with $\lambda(r, z) = \lambda_0$ (a constant), that is, the low conducting interface Γ_0 is homogeneous.

The exact solution of this specific problem is

$$T(r, z) = \sigma_i + \tau_i \ln(r) \text{ for } (r, z) \in \Omega_i \ (i = 1, 2),$$

where

$$\begin{aligned}
\sigma_1 &= T_{\rm a} - \tau_1[\frac{\kappa_1}{cr_{\rm outer}} + \ln(r_{\rm outer})],\ \sigma_2 = T_{\rm c} - \tau_2 \ln(r_{\rm inner}),\\
\tau_1 &= \frac{\kappa_2}{\kappa_1}\tau_2,\ \tau_2 = \frac{\lambda_0}{\chi}(T_{\rm a} - T_{\rm c}),\\
\chi &= \frac{k_2}{r_{\rm int}} - \lambda_0[\ln(r_{\rm inner}) - \frac{\kappa_2}{\kappa_1}(\ln(r_{\rm outer}) + \frac{\kappa_1}{cr_{\rm outer}}) - (1 - \frac{\kappa_2}{\kappa_1})\ln(r_{\rm int})].
\end{aligned}$$

For the purpose of testing the boundary element procedure in Section 4, take $h = 1$, $r_{\rm outer} = 3/2$, $r_{\rm int} = 1$, $r_{\rm inner} = 1/2$, $\kappa_1 = 1/2$, $\kappa_2 = 3/4$, $\lambda_0 = 10$, $c = 1$, $T_{\rm a} = 1$ and $T_{\rm c} = 5$. The exterior boundary of $\Omega_1 \cup \Omega_2$ and the interface Γ_0 are approximated as straight lines with $2N_0$ sides (so that $N = 8N_0$ and $M = 2N_0$).

Equations (19) and (20) are solved using $N_0 = 5$, 10, 20 and 30 and the numerical values of T at various selected points in $\Omega_1 \cup \Omega_2$ as computed by using (11) with $\gamma(\underline{\mathbf{x}}_0) = 1$ are compared with the exact values in Table 1. The numerical values are in good agreement with the exact ones and they converge to the exact solution when N_0 is increased from 5 to 30 (that is, when the calculation is refined by reducing the sizes of the boundary elements used).

Table 1. A comparison of the numerical values of T with the exact solution at various selected points.

Point	$N_0 = 5$	$N_0 = 10$	$N_0 = 20$	$N_0 = 30$	Exact
(0.600,0.100)	4.616703	4.613403	4.612124	4.611786	4.611326
(0.750,0.500)	4.139119	4.137097	4.136263	4.136022	4.135628
(0.900,0.900)	3.754166	3.750142	3.748390	3.747864	3.746954
(1.250,0.750)	2.652760	2.650462	2.649568	2.649317	2.648913
(1.100,0.100)	3.061885	3.059512	3.058493	3.058192	3.057687
(1.490,0.100)	2.094195	2.089170	2.087941	2.087660	2.087292

As expected, for a given N_0, the numerical value of the temperature jump ΔT is found to have approximately the same value on all the elements of the interface Γ_0. Moreover, the percentage errors in the numerical values of ΔT are around 0.92%, 0.45%, 0.22% and 0.15% for N_0 given by 5, 10, 20 and 30 respectively.

Problem 2. Problem 1 deals with one-dimensional heat conduction across a homogeneous interface. For a more general test problem involving the low conducting interface conditions (3) with coefficient λ which varies in space, take

$$\begin{aligned} \Omega_1 &= \{(r,z):\ 0 \le r < 1,\ 0 < z < 1\}, \\ \Omega_2 &= \{(r,z):\ 0 \le r < 1,\ 1 < z < 2\}. \end{aligned}$$

together with $\lambda = 1/(1+r^2)$, $\kappa_1 = 1/4$, $\kappa_2 = 1$ and the boundary conditions

$$\left.\begin{aligned} P(r,0;0,-1) &= 0 \\ T(r,2) &= -4 \end{aligned}\right\} \text{ for } 0 < r < 1,$$

$$P(1,z;1,0) = \begin{cases} 2 & \text{for} \quad 0 < z < 1, \\ 0 & \text{for} \quad 1 < z < 2. \end{cases}$$

Note that the interface between Ω_1 and Ω_2 is given by $0 \le r < 1$, $z = 1$. Refer to Figure 3.

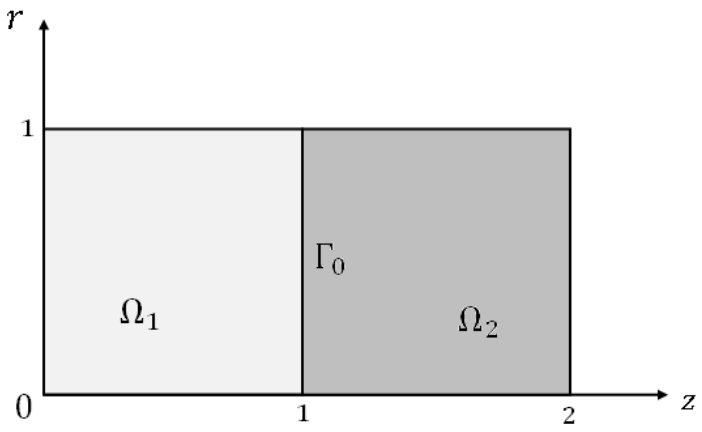

Figure 3. A geometrical sketch of Problem 2 on the rz plane.

It may be easily verified that the exact solution for the test problem here is given by

$$T(r,z) = \begin{cases} r^2 - 2z^2 & \text{for} \quad (r,z) \in \Omega_1, \\ -2 - z & \text{for} \quad (r,z) \in \Omega_2. \end{cases}$$

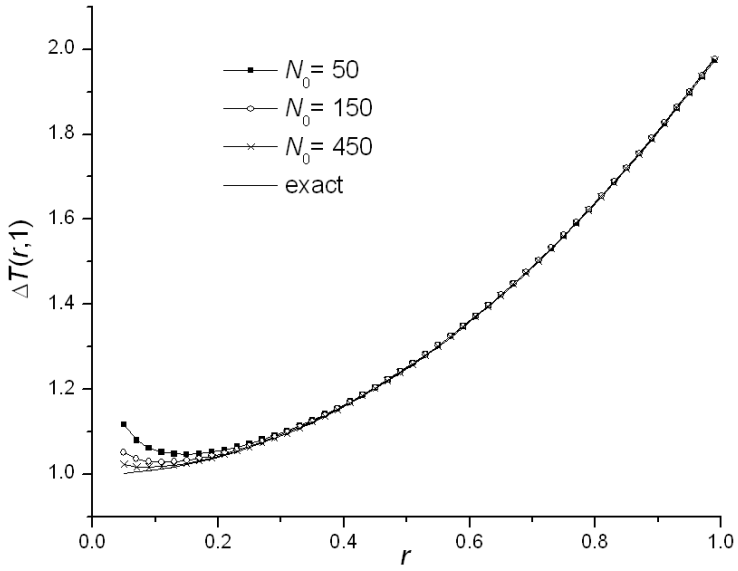

Figure 4. Plots of the numerical and exact temperature jump $\Delta T(r, 1)$ for $0.05 \leq r \leq 0.95$.

For the problem here, each of Γ_1 and Γ_2 comprises two straight line segments of unit length on the rz plane. The interface Γ_0 is a vertical line segment of unit length. To obtain some numerical results, each of the unit length line segments is discretized into N_0 equal length boundary elements (so that $N = 4N_0$ and $M = N_0$). Three sets of numerical values are obtained for $\Delta T(r, 1)$ across the interface Γ_0 by solving the equations (19) and (20) using $N_0 = 50, 150$ and 450. Figure 4 compares the numerical $\Delta T(r, 1)$ with the values obtained from the exact solution for $0.05 \leq r \leq 0.95$. On the whole, there is a good agreement between the numerical and exact temperature jump, except for points which are very close to $r = 0$. Nevertheless, as clearly shown in Figure 4, the errors for the temperature jump for r close to zero are significantly reduced when the number of boundary and interface elements is increased.

As the temperature is not known a priori on the boundary $r = 1(0 < z < 2)$, the numerical values of the boundary temperature $T(1, z)$ are compared graphically with the exact temperature in Figure 5. The numerical and exact temperature agree well with each other. Note the gap in the graph is due to

the temperature jump across the interface Γ_0 at $z = 1$.

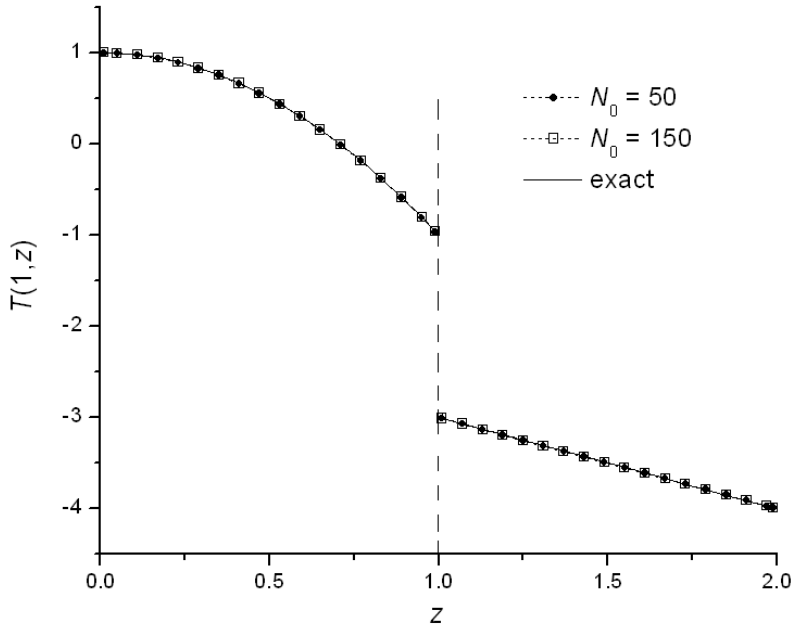

Figure 5. Plots of the numerical and exact boundary temperature $T(1, z)$ for $0 < z < 2$.

Problem 3. Consider now a homogeneous cylindrical representative volume element containing a centrally located cylindrical carbon nanotube as in Ang, Singh and Tanaka [3]. The regions Ω_1 and Ω_2 are as sketched in Figure 6. As the carbon nanotube is centrally located in the composite, the lengths ℓ_1, ℓ_2 and ℓ_3 are such that $\ell_1 + \ell_2 = \ell_3$. Here Ω_1 is taken to be occupied by elastomer S160 with thermal conductivity $\kappa_1 = 0.56$ $\mathrm{Wm^{-1}K^{-1}}$ and Ω_2 is occupied by the carbon nanotube whose thermal conductivity κ_2 is taken to be given by 6000 $\mathrm{Wm^{-1}K^{-1}}$.

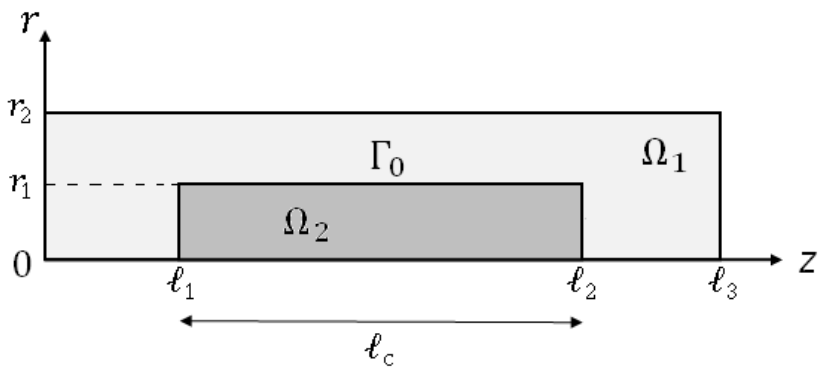

Figure 6. A geometrical sketch of Problem 3 on the rz plane.

The boundary conditions on the exterior of Ω_1 are given by

$$\left.\begin{array}{r} T(r,0) = 200 \text{ K} \\ T(r,\ell_3) = 100 \text{ K} \end{array}\right\} \text{for } 0 < r < r_2,$$
$$P(r_2, z; 1, 0) = 0 \text{ for } 0 < z < \ell_3.$$

Of interest here is to examine the effect of the interfacial parameter λ (assumed to be a constant) on the equivalent (effective) thermal conductivity $\kappa_{\rm e}$ of the carbon nanotube based composite along the z direction. In Ang, Singh and Tanaka [3], the equivalent thermal conductivity $\kappa_{\rm e}$ is calculated for the limiting case $\lambda \to \infty$ (that is, the case in which the interface between the elastomer and the carbon nanotube is perfectly conducting) by modeling the carbon nanotube as a thermal superconductor.

The equivalent thermal conductivity $\kappa_{\rm e}$ is given by

$$\kappa_{\rm e} = -\frac{q_{\rm ave}\ell_3}{T(r,\ell_3) - T(r,0)},$$

where $q_{\rm ave}$ is the average heat flux across $0 \le r < r_2$, $z = \ell_3$. The average heat flux can be calculated approximately from the numerical solution in Section 4 by using

$$q_{\rm ave} \simeq -\frac{2\kappa_1}{r_2^2} \sum_{k=1}^{J} P^{(k)} \{ r^{(k)} \ell^{(k)} + \frac{1}{2} (\ell^{(k)})^2 \},$$

if the side $z = \ell_3$ for $0 \leq r \leq r_2$ (on the rz plane) is discretized into J elements denoted by $C^{(1)}$, $C^{(2)}$, $\cdots$, $C^{(J-1)}$ and $C^{(J)}$.

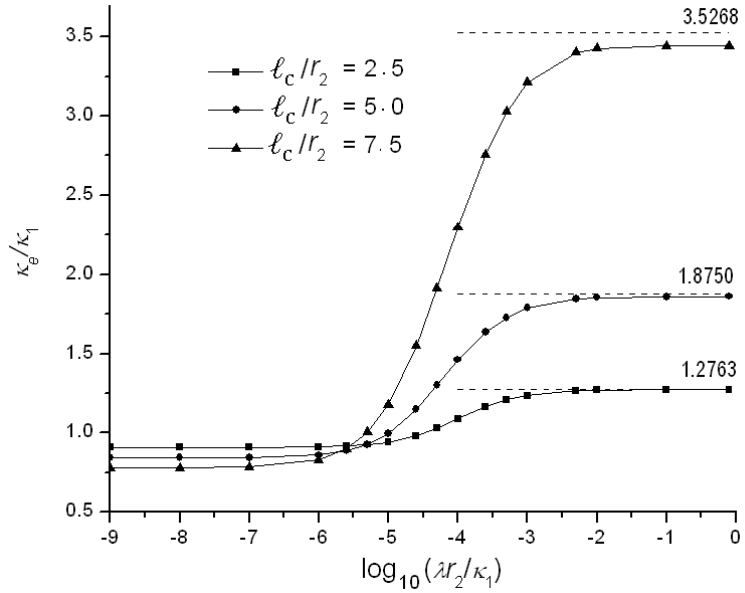

Figure 7. Plots of κ_e/κ_1 against $\log_{10}(\lambda r_2/\kappa_1)$ for a few selected values of ℓ_c/r_2. Horizontal dashed lines give values of κ_e/κ_1 as calculated in Ang, Singh and Tanaka [3] for the case in which the interface between the elastomer and the carbon nanotube is ideal.

The radii r_1 and r_2 and the lengths ℓ_1, ℓ_2 and ℓ_3 are taken to be such that $r_1/r_2 = 1/2$ and $(\ell_1 + \ell_2)/r_2 = \ell_3/r_2 = 10$. To calculate the non-dimensionalized equivalent thermal conductivity κ_e/κ_1, as many as 3600 elements are employed on the exterior boundary and interface of the carbon nanotube composite. Figure 7 gives plots of κ_e/κ_1 against $\log_{10}(\lambda r_2/\kappa_1)$ for some selected values of the non-dimensionalized length ℓ_c/r_2 of the carbon nanotube. The non-dimensionalized equivalent thermal conductivity κ_e/κ_1 is found to be less than 1 for $\lambda r_2/\kappa_1$ which is very close to zero. This is expected, because if the interface between the elastomer and the carbon nanotube is highly damaged, the carbon nanotube behaves as a thermal insulator which obstructs the flow of heat. From Figure 7, it is obvious that κ_e/κ_1 tends to a

lower value as $\lambda r_2/\kappa_1$ approaches 0 (from above) for larger ℓ_c/r_2 (that is, for a longer carbon nanotube). As $\lambda r_2/\kappa_1$ increases in magnitude, the carbon nanotube serves to enhance the flow of heat through the composite. Thus, κ_e/κ_1 is greater than 1 for larger $\lambda r_2/\kappa_1$. In Figure 7, the values of κ_e/κ_1 calculated in [3] for the case in which the interface between the elastomer and the carbon nanotube is perfectly conducting are shown using horizontal dashed lines. For a given ℓ_c/r_2, it appears that κ_e/κ_1 becomes closer but is less than the value given by dashed line, as $\lambda r_2/\kappa_1$ increases. As may be expected, for a larger value of ℓ_c/r_2, the difference between the lower and the upper bounds of κ_e/κ_1 is bigger.

Problem 4.

To check the boundary element procedure for the high conducting interfacial conditions (4), consider the regions Ω_1 and Ω_2 as sketched in Figure 8. Note that Ω_1 and Ω_2 are defined by the curves $r^2 + z^2 = 9/4$, $r^2 + z^2 = 1$ and $r^2 + z^2 = 1/4$ and the lines $r = 0$ and $r = (\sqrt{3}/3)z$ on the rz plane.

For a particular problem, take $\kappa_1 = 3/4$ and $\kappa_2 = 1/2$. The interface Γ_0 between the two regions is high conducting with

$$\alpha = \frac{r^2 - 2z^2}{4(2r^2 - z^2)}.$$

The boundary conditions on the exterior boundary of $\Omega_1 \cup \Omega_2$ are given by

$$\begin{aligned}
P(r, z; \frac{2}{3}r, \frac{2}{3}z) &= \frac{4}{3}(r^2 - 2z^2) \text{ for } r^2 + z^2 = \frac{9}{4},\ 0 < r < \frac{\sqrt{3}}{3}z, \\
T(r, z) &= 2r^2 - \frac{9}{4} \text{ for } r^2 + z^2 = \frac{1}{4},\ 0 < r < \frac{\sqrt{3}}{3}z, \\
T(r, z) &= -\frac{2}{3}z^2 \text{ for } r = \frac{\sqrt{3}}{3}z,\ \frac{1}{4} < r^2 + z^2 < 1, \\
T(r, z) &= -\frac{2}{3}z^2 \text{ for } r = \frac{\sqrt{3}}{3}z,\ 1 < r^2 + z^2 < \frac{9}{4}.
\end{aligned}$$

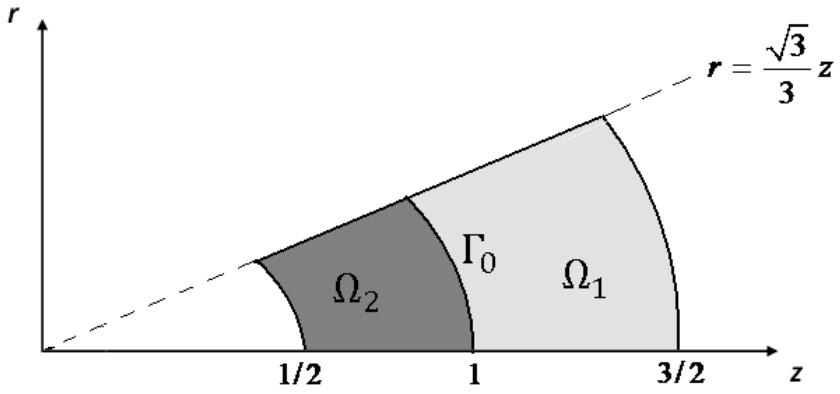

Figure 8. A geometrical sketch of Problem 4 on the rz plane.

For the purpose of obtaining some numerical results, the the interface Γ_0 is discretized into $2N_0$ elements and the exterior boundary into $5N_0$ elements (hence $N = 5N_0$ and $M = 2N_0$). Equations (27), (28) and (34) are then solved as a system of $9N_0$ linear algebraic equations with $N_0 = 5$, 10, 20 and 40. The largest elements for $N_0 = 5$, 10, 20 and 40 have magnitudes of 0.10, 0.05, 0.025 and 0.0125 units respectively. The numerically computed temperature at various selected points in $\Omega_1 \cup \Omega_2$ are then compared with the exact solution given by

$$T(r, z) = r^2 - z^2 \text{ for } (r, z) \in \Omega_1 \cup \Omega_2.$$

Table 2. Numerical and exact values of T at selected interior points.

Point	$N_0 = 5$	$N_0 = 10$	$N_0 = 20$	$N_0 = 40$	Exact
$(0.10, 0.60)$	-0.709956	-0.709985	-0.709982	-0.709995	-0.71000
$(0.20, 0.70)$	-0.940185	-0.940049	-0.939990	-0.939999	-0.94000
$(0.45, 0.80)$	-1.098310	-1.080885	-1.076857	-1.077520	-1.07750
$(0.50, 0.90)$	-1.382515	-1.368887	-1.370157	-1.370010	-1.37000
$(0.20, 1.10)$	-2.378008	-2.379544	-2.379830	-2.380000	-2.38000
$(0.10, 1.40)$	-3.904657	-3.908711	-3.909656	-3.909920	-3.91000

As shown in Table 2, the numerical values for T are reasonably accurate and they converge to the exact solution when the calculation is refined by increasing the number of elements used. All percentage errors of the numerical values for $N_0 = 40$ are less than 0.01%.

Problem 5.

Consider now a thermal management system comprising a computer chip and a heat sink modeled by two homogeneous cylindrical solids. In addition, the cylindrical solids are joined together by a thin layer of carbon nanotubes or nanocylinders of high thermal conductivity. Such an interface may be modeled as high conducting. The regions Ω_1 and Ω_2 as sketched in Figure 9 are respectively the heat sink and the computer chip. The line $z = z_1$, $0 < r < r_1$, denoted by Γ_0, is the high conducting interface.

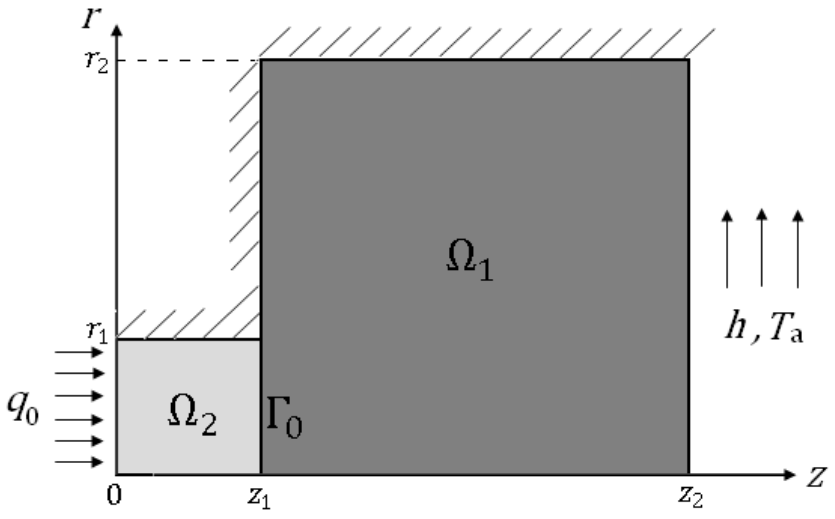

Figure 9. A geometrical sketch of Problem 5 on the rz plane.

Except for the sides $z = 0$, $0 < r < r_1$ (where a constant heat flux q_0 flows into the system) and $z = z_2$, $0 < r < r_2$ (where there is a uniform convective cooling), the exterior boundary of the bimaterial thermal system is thermally

insulated. More specifically, the boundary conditions on the sides that are not thermally insulated are as follows:

$$\begin{aligned} -\kappa_2 P(r,0;0,-1) &= q_0 \text{ for } 0<r<r_1, \\ -\kappa_1 P(r,z_2;0,1) &= h[T(r,z_2)-T_{\mathrm{a}}] \text{ for } 0<r<r_2, \end{aligned}$$

where h is the heat convection coefficient, q_0 is the magnitude of the specified heat flux and T_{a} is the ambient temperature of the system.

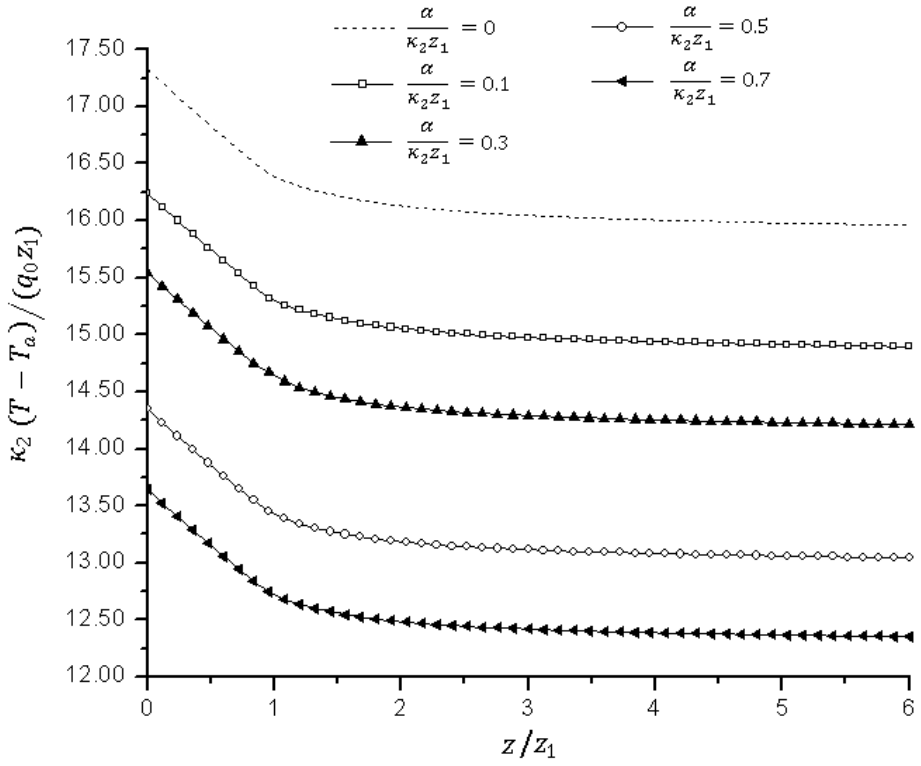

Figure 10. Plots of $\kappa_2(T-T_{\mathrm{a}})/(q_0 z_1)$ against z/z_1 for a few selected values of $\alpha/(\kappa_2 z_1)$ (for perfectly conducting and high conducting interfaces).

We are interested in analyzing the effect of the interfacial parameter α (assumed to be constant) on the thermal performance of the heat dissipation system. The radii r_1 and r_2 and the lengths z_1 and z_2 are chosen to

be such that $r_2/r_1 = 5$ and $(z_2 - z_1)/z_1 = 5$. To obtain some numerical results, a total of 2880 elements are employed on the exterior boundary of $\Omega_1 \cup \Omega_2$ and the interface Γ_0. For $hz_1/\kappa_2 = 2.5 \times 10^{-3}$ and $\kappa_1/\kappa_2 = 2.20$, the non-dimensionalized temperature $\kappa_2(T - T_\mathrm{a})/(q_0 z_1)$ along the z-axis are plotted against z/z_1 for selected values of the non-dimensionalized parameter $\alpha/(\kappa_2 z_1)$.

In Figure 10, the dashed line gives the plot of the non-dimensionalized temperature profile for the case in which the interface between the chip and heat sink is perfectly bonded (that is, for the case $\alpha/(\kappa_2 z_1) = 0$). As anticipated, at a given point on the z axis, the non-dimensionalized temperature in both the computer chip and heat sink decreases as $\alpha/(\kappa_2 z_1)$ increases. Hence, high conducting interfaces enhance the heat dissipation performance of the system.

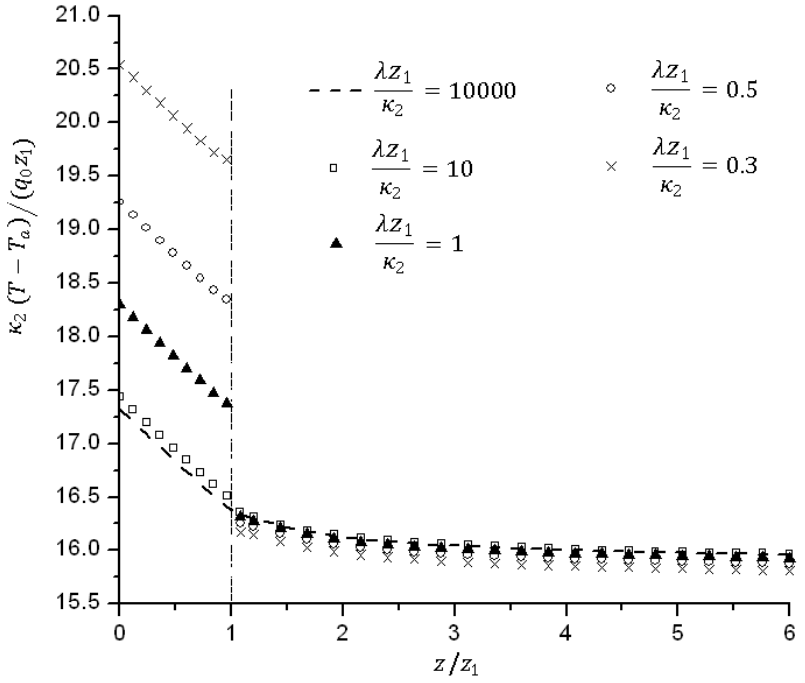

Figure 11. Plots of $\kappa_2(T - T_\mathrm{a})/(q_0 z_1)$ against z/z_1 for a few selected values of $\lambda z_1/\kappa_2$ (for low conducting interfaces).

Still with $r_2/r_1 = 5$, $(z_2 - z_1)/z_1 = 5$, $hz_1/\kappa_2 = 2.5 \times 10^{-3}$ and $\kappa_1/\kappa_2 = 2.20$, we plot $\kappa_2(T - T_a)/(q_0 z_1)$ against z_1/z for the case in which the interface between the chip and the sink is a low conducting one. The plots for selected values of the non-dimensionalized parameter $\lambda z_1/\kappa_2$ are given in Figure 11. As the low conducting interface tends to obstruct rather than enhance heat flow from the chip into the sink, the temperature profiles in the chip in Figure 11 are higher compared to those in Figure 10. As expected, for a lower value of $\lambda z_1/\kappa_2$, there is a bigger temperature jump across the interface at $z/z_1 = 1$.The differences between the temperature distributions for the different values of $\lambda z_1/\kappa_2$ are much smaller in the sink compared to those in the chip.

The effects of the three types of interfaces-low conducting, perfectly conducting and high conducting ones-on the thermal performance of the heat disspipation system in Figure 9 are clearly shown by the temperature profiles in Figures 10 and 11.

7 Conclusion and summary

Boundary integral formulations for axisymmetric heat conduction across low conducting and high conducting interfaces between two dissimilar materials are derived. A simple boundary element procedure based on these formulations is proposed for solving numerically the axisymmetric heat conduction problem. To assess the validity and accuracy of the numerical procedure, it is used to solve some specific test problems which have analytical (exact) solutions. The numerical solutions obtained suggest that the boundary integral formulations are correctly derived and the proposed numerical procedure can be used as an accurate and reliable tool for analyzing heat flow across the non-ideal interfaces.

The boundary element procedure is also applied to solve some problems of practical interest. One of the problems requires the computation of the equivalent thermal conductivity of a homogeneous cylindrical representative volume element containing a centrally located cylindrical carbon nanotube. The interface between the constituent parts of the carbon nanotube based composite is assumed to be microscopically damaged and is modeled as low conducting. In another problem, the thermal performance of a heat dissipa-

tion system comprising a computer chip and a heat sink is simulated. The effects of both low and high conducting interfaces (between the chip and the sink) on the temperature distribution in the thermal system are examined. The numerical results obtained for the equivalent thermal conductivity of the carbon nanotube composite and the temperature profiles in the computer chip and the heat sink appear to be intuitively and qualitatively acceptable. Heat conduction is shown to be impeded across a low conducting interface and enhanced across a high conducting interface.

References

[1] W. T. Ang, A hypersingular boundary integral formulation for heat conduction across a curved imperfect interface, *Communications in Numerical Methods in Engineering* **24** (2008) 841-851.

[2] W. T. Ang, K. K. Choo and H. Fan, A Green's function for steady-state two-dimensional isotropic heat conduction across a homogeneously imperfect interface, *Communications in Numerical Methods in Engineering* **20** (2004) 391-399.

[3] W. T. Ang, I.V. Singh and M. Tanaka, An axisymmetric heat conduction model for a multi-material cylindrical system with application to analysis of carbon nanotube based composites, *International Journal of Engineering Science* **45** (2007) 22-33.

[4] Y. Benveniste, On the decay of end effects in conduction phenomena: A sandwich strip with imperfect interfaces of low or high conductivity, *Journal of Applied Physics* **86** (1999) 1273-1279.

[5] Y. Benveniste and T. Miloh, Imperfect soft and stiff interfaces in two-dimensional elasticity, *Mechanics of Materials* **33** (2001) 309-323.

[6] C. A. Brebbia, J. C. F. Telles and L. C. Wrobel, *Boundary Element Techniques, Theory and Applications in Engineering*, Springer-Verlag, Berlin/Heidelberg, 1984.

[7] A. Desai, J. Geer and B. Sammakia, Models of steady heat conduction in multiple cylindrical domains, *Journal of Electronic Packaging-Transactions of the ASME* **128** (2006) 10-17.

[8] T. Miloh and Y. Benveniste, On the effective conductivity of composites with ellipsoidal inhomogeneities and highly conducting interfaces, *Proceedings of the Royal Society of London Series A-Mathematical, Physical and Engineering Sciences* **455** (1999) 2687-2706.

[9] E. T. Whittaker and G. N. Watson, *A Course in Modern Analysis*, Cambridge University Press, Cambridge, 1990.

Appendix

More explicitly, the function $\Lambda_0(\underline{\mathbf{x}};\underline{\mathbf{x}}_0;\underline{\mathbf{t}}^{(i)})$ in (31) is given by

$$\begin{aligned}
&\Lambda_0(\underline{\mathbf{x}};\underline{\mathbf{x}}_0;\underline{\mathbf{t}}^{(i)}) \\
= \;& \frac{1}{\pi\sqrt{a(\underline{\mathbf{x}};\underline{\mathbf{x}}_0)+b(r;r_0)}(a(\underline{\mathbf{x}};\underline{\mathbf{x}}_0)-b(r;r_0))^2} \\
&\times\{t_r^{(i)}Y_1(\underline{\mathbf{x}};\underline{\mathbf{x}}_0;\underline{\mathbf{t}}^{(i)})+t_z^{(i)}Y_2(\underline{\mathbf{x}};\underline{\mathbf{x}}_0;\underline{\mathbf{t}}^{(i)})\},
\end{aligned} \tag{A1}$$

where

$$\begin{aligned}
&Y_1(\underline{\mathbf{x}};\underline{\mathbf{x}}_0;\underline{\mathbf{t}}^{(i)}) \\
= \;& (r+r_0)(1-m(\underline{\mathbf{x}};\underline{\mathbf{x}}_0))[\frac{t_r^{(i)}}{2r_0}[\left(a(\underline{\mathbf{x}};\underline{\mathbf{x}}_0)-2r_0^2\right)E(m(\underline{\mathbf{x}};\underline{\mathbf{x}}_0)) \\
&-(a(\underline{\mathbf{x}};\underline{\mathbf{x}}_0)-b(r;r_0))K(m(\underline{\mathbf{x}};\underline{\mathbf{x}}_0))]+t_z^{(i)}(z-z_0)E(m(\underline{\mathbf{x}};\underline{\mathbf{x}}_0))] \\
&-\frac{t_r^{(i)}}{2r_0^2}[(a(\underline{\mathbf{x}};\underline{\mathbf{x}}_0)-b(r;r_0))^2K(m(\underline{\mathbf{x}};\underline{\mathbf{x}}_0))-\left(a(\underline{\mathbf{x}};\underline{\mathbf{x}}_0)-2r_0^2\right) \\
&\times(a(\underline{\mathbf{x}};\underline{\mathbf{x}}_0)-b(r;r_0))E(m(\underline{\mathbf{x}};\underline{\mathbf{x}}_0))-r_0\left(a(\underline{\mathbf{x}};\underline{\mathbf{x}}_0)-2r_0^2\right) \\
&\times(1-m(\underline{\mathbf{x}};\underline{\mathbf{x}}_0))\left[(r+r_0)E(m(\underline{\mathbf{x}};\underline{\mathbf{x}}_0))+(r-r_0)K(m(\underline{\mathbf{x}};\underline{\mathbf{x}}_0))\right] \\
&+2r_0E(m(\underline{\mathbf{x}};\underline{\mathbf{x}}_0))[r(a(\underline{\mathbf{x}};\underline{\mathbf{x}}_0)-b(r;r_0))-2r_0\left(z-z_0\right)^2]] \\
&-t_z^{(i)}(z-z_0)[\frac{1}{2r_0}\left(1-m(\underline{\mathbf{x}};\underline{\mathbf{x}}_0)\right)\left(a(\underline{\mathbf{x}};\underline{\mathbf{x}}_0)-2r_0^2\right) \\
&\times\left(E(m(\underline{\mathbf{x}};\underline{\mathbf{x}}_0))-K(m(\underline{\mathbf{x}};\underline{\mathbf{x}}_0))\right)+2(r-r_0)E(m(\underline{\mathbf{x}};\underline{\mathbf{x}}_0))],
\end{aligned} \tag{A2}$$

and

$$
\begin{aligned}
& Y_2(\underline{\mathbf{x}};\underline{\mathbf{x}}_0;\underline{\mathbf{t}}^{(i)}) \\
= \; & -\{(z-z_0)\,(1-m(\underline{\mathbf{x}};\underline{\mathbf{x}}_0))\,[\frac{t_r^{(i)}}{2r_0}[\left(a(\underline{\mathbf{x}};\underline{\mathbf{x}}_0)-2r_0^2\right)E(m(\underline{\mathbf{x}};\underline{\mathbf{x}}_0)) \\
& -(a(\underline{\mathbf{x}};\underline{\mathbf{x}}_0)-b(r;r_0))K(m(\underline{\mathbf{x}};\underline{\mathbf{x}}_0))]+t_z^{(i)}(z-z_0)E(m(\underline{\mathbf{x}};\underline{\mathbf{x}}_0))] \\
& +t_r^{(i)}(z-z_0)[2(r-r_0)E(m(\underline{\mathbf{x}};\underline{\mathbf{x}}_0))-(1-m(\underline{\mathbf{x}};\underline{\mathbf{x}}_0)) \\
& \times[(r+r_0)E(m(\underline{\mathbf{x}};\underline{\mathbf{x}}_0))+(r-r_0)K(m(\underline{\mathbf{x}};\underline{\mathbf{x}}_0))]] \\
& +t_z^{(i)}[(z-z_0)^2\,[(2-m(\underline{\mathbf{x}};\underline{\mathbf{x}}_0))\,E(m(\underline{\mathbf{x}};\underline{\mathbf{x}}_0)) \\
& -(1-m(\underline{\mathbf{x}};\underline{\mathbf{x}}_0))\,K(m(\underline{\mathbf{x}};\underline{\mathbf{x}}_0))]-(r-r_0)^2\,E(m(\underline{\mathbf{x}};\underline{\mathbf{x}}_0))]\}. \qquad \text{(A3)}
\end{aligned}
$$

The partial derivatives defining the function $\Lambda_1(\underline{\mathbf{x}};\underline{\mathbf{x}}_0;\underline{\mathbf{n}}^{(k)};\underline{\mathbf{t}}^{(i)})$ are explicitly given by

$$
\begin{aligned}
& \frac{\partial}{\partial r_0}[\Phi_1(\underline{\mathbf{x}};\underline{\mathbf{x}}_0;\underline{\mathbf{n}}^{(k)};\underline{\mathbf{t}}^{(i)})] \\
= \; & \frac{1}{\pi\sqrt{a(\underline{\mathbf{x}};\underline{\mathbf{x}}_0)+b(r;r_0)}(a(\underline{\mathbf{x}};\underline{\mathbf{x}}_0)-b(r;r_0))^2} \\
& \times\{\frac{4(r-r_0)(a(\underline{\mathbf{x}};\underline{\mathbf{x}}_0)+b(r;r_0))-(r+r_0)(a(\underline{\mathbf{x}};\underline{\mathbf{x}}_0)-b(r;r_0))}{(a(\underline{\mathbf{x}};\underline{\mathbf{x}}_0)+b(r;r_0))(a(\underline{\mathbf{x}};\underline{\mathbf{x}}_0)-b(r;r_0))} \\
& \times[t_r^{(i)}\Theta(\underline{\mathbf{x}};\underline{\mathbf{x}}_0;\underline{\mathbf{n}}^{(k)})+t_z^{(i)}\Psi(\underline{\mathbf{x}};\underline{\mathbf{x}}_0;\underline{\mathbf{n}}^{(k)})] \\
& +[t_r^{(i)}Y_3(\underline{\mathbf{x}};\underline{\mathbf{x}}_0;\underline{\mathbf{n}}^{(k)})+t_z^{(i)}Y_4(\underline{\mathbf{x}};\underline{\mathbf{x}}_0;\underline{\mathbf{n}}^{(k)})]\} \qquad \text{(A4)}
\end{aligned}
$$

and

$$
\begin{aligned}
& \frac{\partial}{\partial z_0}[\Phi_1(\underline{\mathbf{x}};\underline{\mathbf{x}}_0;\underline{\mathbf{n}}^{(k)};\underline{\mathbf{t}}^{(i)})] \\
= \; & \frac{1}{\pi\sqrt{a(\underline{\mathbf{x}};\underline{\mathbf{x}}_0)+b(r;r_0)}(a(\underline{\mathbf{x}};\underline{\mathbf{x}}_0)-b(r;r_0))^2} \\
& \times\{\frac{(z-z_0)[5(a(\underline{\mathbf{x}};\underline{\mathbf{x}}_0)+b(r;r_0))-4rr_0]}{(a(\underline{\mathbf{x}};\underline{\mathbf{x}}_0)+b(r;r_0))(a(\underline{\mathbf{x}};\underline{\mathbf{x}}_0)-b(r;r_0))} \\
& \times[t_r^{(i)}\Theta(\underline{\mathbf{x}};\underline{\mathbf{x}}_0;\underline{\mathbf{n}}^{(k)})+t_z^{(i)}\Psi(\underline{\mathbf{x}};\underline{\mathbf{x}}_0;\underline{\mathbf{n}}^{(k)})] \\
& +[t_r^{(i)}Y_5(\underline{\mathbf{x}};\underline{\mathbf{x}}_0;\underline{\mathbf{n}}^{(k)})+t_z^{(i)}Y_6(\underline{\mathbf{x}};\underline{\mathbf{x}}_0;\underline{\mathbf{n}}^{(k)})]\} \qquad \text{(A5)}
\end{aligned}
$$

where

$$
\begin{aligned}
&Y_3(\underline{\mathbf{x}};\underline{\mathbf{x}}_0;\underline{\mathbf{n}}^{(k)}) = [(1-m(\underline{\mathbf{x}};\underline{\mathbf{x}}_0)) - \frac{m(\underline{\mathbf{x}};\underline{\mathbf{x}}_0)(r+r_0)\left(a(\underline{\mathbf{x}};\underline{\mathbf{x}}_0)-2r_0^2\right)}{r_0(a(\underline{\mathbf{x}};\underline{\mathbf{x}}_0)+b(r;r_0))}]\\
&\times\{\frac{n_r^{(k)}}{2r}[\left(a(\underline{\mathbf{x}};\underline{\mathbf{x}}_0)-2r^2\right)E(m(\underline{\mathbf{x}};\underline{\mathbf{x}}_0)) - (a(\underline{\mathbf{x}};\underline{\mathbf{x}}_0)-b(r;r_0))K(m(\underline{\mathbf{x}};\underline{\mathbf{x}}_0))]\\
&-n_z^{(k)}(z-z_0)E(m(\underline{\mathbf{x}};\underline{\mathbf{x}}_0))\} + (r+r_0)\left(1-m(\underline{\mathbf{x}};\underline{\mathbf{x}}_0)\right)\\
&\times\{\frac{n_r^{(k)}}{r}[r_0E(m(\underline{\mathbf{x}};\underline{\mathbf{x}}_0)) + (r-r_0)K(m(\underline{\mathbf{x}};\underline{\mathbf{x}}_0))]\\
&+\frac{(a(\underline{\mathbf{x}};\underline{\mathbf{x}}_0)-2r_0^2)}{2r_0(a(\underline{\mathbf{x}};\underline{\mathbf{x}}_0)+b(r;r_0))}\\
&\times\left(n_r^{(k)}[(r-r_0)K(m(\underline{\mathbf{x}};\underline{\mathbf{x}}_0)) - (r+r_0)E(m(\underline{\mathbf{x}};\underline{\mathbf{x}}_0))]\right.\\
&\left.-n_z^{(k)}(z-z_0)(E(m(\underline{\mathbf{x}};\underline{\mathbf{x}}_0)) - K(m(\underline{\mathbf{x}};\underline{\mathbf{x}}_0)))\right)\}\\
&-n_r^{(k)}\{-\frac{(1-m(\underline{\mathbf{x}};\underline{\mathbf{x}}_0))\,a(\underline{\mathbf{x}};\underline{\mathbf{x}}_0)}{2r_0^2}[(r-r_0)K(m(\underline{\mathbf{x}};\underline{\mathbf{x}}_0))\\
&-(r+r_0)E(m(\underline{\mathbf{x}};\underline{\mathbf{x}}_0))] + 2(r+r_0)E(m(\underline{\mathbf{x}};\underline{\mathbf{x}}_0))\\
&+\frac{\left(a(\underline{\mathbf{x}};\underline{\mathbf{x}}_0)-2r_0^2\right)^2}{4r_0^2(a(\underline{\mathbf{x}};\underline{\mathbf{x}}_0)+b(r;r_0))}\\
&\times[[(3m(\underline{\mathbf{x}};\underline{\mathbf{x}}_0)-1)(r+r_0)+(r-r_0)]E(m(\underline{\mathbf{x}};\underline{\mathbf{x}}_0))\\
&+2(r_0-m(\underline{\mathbf{x}};\underline{\mathbf{x}}_0)r)K(m(\underline{\mathbf{x}};\underline{\mathbf{x}}_0))] - \frac{(a(\underline{\mathbf{x}};\underline{\mathbf{x}}_0)-2r_0^2)}{r_0(a(\underline{\mathbf{x}};\underline{\mathbf{x}}_0)+b(r;r_0))}\\
&\times[(r-r_0)^2E(m(\underline{\mathbf{x}};\underline{\mathbf{x}}_0)) + (z-z_0)^2K(m(\underline{\mathbf{x}};\underline{\mathbf{x}}_0))]\}\\
&+n_z^{(k)}(z-z_0)\{\frac{(E(m(\underline{\mathbf{x}};\underline{\mathbf{x}}_0)) - K(m(\underline{\mathbf{x}};\underline{\mathbf{x}}_0)))\left(a(\underline{\mathbf{x}};\underline{\mathbf{x}}_0)-2r_0^2\right)(r-r_0)}{r_0(a(\underline{\mathbf{x}};\underline{\mathbf{x}}_0)+b(r;r_0))}\\
&-2E(m(\underline{\mathbf{x}};\underline{\mathbf{x}}_0)) + \frac{\left(a(\underline{\mathbf{x}};\underline{\mathbf{x}}_0)-2r_0^2\right)^2}{4r_0^2(a(\underline{\mathbf{x}};\underline{\mathbf{x}}_0)+b(r;r_0))}\\
&\times[m(\underline{\mathbf{x}};\underline{\mathbf{x}}_0)(2K(m(\underline{\mathbf{x}};\underline{\mathbf{x}}_0)) - 3E(m(\underline{\mathbf{x}};\underline{\mathbf{x}}_0)))]\\
&-\frac{(1-m(\underline{\mathbf{x}};\underline{\mathbf{x}}_0))\,a(\underline{\mathbf{x}};\underline{\mathbf{x}}_0)}{2r_0^2}(E(m(\underline{\mathbf{x}};\underline{\mathbf{x}}_0)) - K(m(\underline{\mathbf{x}};\underline{\mathbf{x}}_0)))\}, \qquad \text{(A6)}
\end{aligned}
$$

$$
\begin{aligned}
& Y_4(\underline{\mathbf{x}};\underline{\mathbf{x}}_0;\underline{\mathbf{n}}^{(k)}) \\
= \; & -(z-z_0)\{(1-m(\underline{\mathbf{x}};\underline{\mathbf{x}}_0))\,\frac{n_r^{(k)}}{r} \\
& \times[r_0E(m(\underline{\mathbf{x}};\underline{\mathbf{x}}_0))+(r-r_0)K(m(\underline{\mathbf{x}};\underline{\mathbf{x}}_0))] \\
& +\frac{(a(\underline{\mathbf{x}};\underline{\mathbf{x}}_0)-2r_0^2)}{2r_0(a(\underline{\mathbf{x}};\underline{\mathbf{x}}_0)+b(r;r_0))} \\
& \times\{(1-m(\underline{\mathbf{x}};\underline{\mathbf{x}}_0))\,[n_r^{(k)}\,((r-r_0)K(m(\underline{\mathbf{x}};\underline{\mathbf{x}}_0)) \\
& -(r+r_0)E(m(\underline{\mathbf{x}};\underline{\mathbf{x}}_0))) \\
& -n_z^{(k)}(z-z_0)(E(m(\underline{\mathbf{x}};\underline{\mathbf{x}}_0))-K(m(\underline{\mathbf{x}};\underline{\mathbf{x}}_0)))] \\
& -2m(\underline{\mathbf{x}};\underline{\mathbf{x}}_0)[\frac{n_r^{(k)}}{2r}[\left(a(\underline{\mathbf{x}};\underline{\mathbf{x}}_0)-2r^2\right)E(m(\underline{\mathbf{x}};\underline{\mathbf{x}}_0)) \\
& -(a(\underline{\mathbf{x}};\underline{\mathbf{x}}_0)-b(r;r_0))K(m(\underline{\mathbf{x}};\underline{\mathbf{x}}_0))] \\
& -n_z^{(k)}(z-z_0)E(m(\underline{\mathbf{x}};\underline{\mathbf{x}}_0))]\}\} \\
& -n_r^{(k)}(z-z_0)\{\frac{(a(\underline{\mathbf{x}};\underline{\mathbf{x}}_0)-2r_0^2)}{2r_0(a(\underline{\mathbf{x}};\underline{\mathbf{x}}_0)+b(r;r_0))} \\
& \times[E(m(\underline{\mathbf{x}};\underline{\mathbf{x}}_0))(3m(\underline{\mathbf{x}};\underline{\mathbf{x}}_0)(r+r_0)-2r) \\
& +K(m(\underline{\mathbf{x}};\underline{\mathbf{x}}_0))(2r\,(1-m(\underline{\mathbf{x}};\underline{\mathbf{x}}_0)))] \\
& -(1-m(\underline{\mathbf{x}};\underline{\mathbf{x}}_0))\,(E(m(\underline{\mathbf{x}};\underline{\mathbf{x}}_0)) \\
& +K(m(\underline{\mathbf{x}};\underline{\mathbf{x}}_0)))+2E(m(\underline{\mathbf{x}};\underline{\mathbf{x}}_0))\} \\
& +n_z^{(k)}\{\frac{(a(\underline{\mathbf{x}};\underline{\mathbf{x}}_0)-2r_0^2)}{2r_0(a(\underline{\mathbf{x}};\underline{\mathbf{x}}_0)+b(r;r_0))} \\
& \times[(z-z_0)^2[(1-3m(\underline{\mathbf{x}};\underline{\mathbf{x}}_0))E(m(\underline{\mathbf{x}};\underline{\mathbf{x}}_0)) \\
& +(2m(\underline{\mathbf{x}};\underline{\mathbf{x}}_0)-1)K(m(\underline{\mathbf{x}};\underline{\mathbf{x}}_0))]-(r-r_0)^2(E(m(\underline{\mathbf{x}};\underline{\mathbf{x}}_0)) \\
& -K(m(\underline{\mathbf{x}};\underline{\mathbf{x}}_0)))]+2(r-r_0)E(m(\underline{\mathbf{x}};\underline{\mathbf{x}}_0))\}, \qquad \text{(A7)}
\end{aligned}
$$

$$
\begin{aligned}
& Y_5(\underline{\mathbf{x}};\underline{\mathbf{x}}_0;\underline{\mathbf{n}}^{(k)}) \\
= \; & [-2m(\underline{\mathbf{x}};\underline{\mathbf{x}}_0)(r+r_0)\frac{(z-z_0)}{a(\underline{\mathbf{x}};\underline{\mathbf{x}}_0)+b(r;r_0)}] \\
& \times\{\frac{n_r^{(k)}}{2r}[\left(a(\underline{\mathbf{x}};\underline{\mathbf{x}}_0)-2r^2\right)E(m(\underline{\mathbf{x}};\underline{\mathbf{x}}_0)) \\
& -(a(\underline{\mathbf{x}};\underline{\mathbf{x}}_0)-b(r;r_0))K(m(\underline{\mathbf{x}};\underline{\mathbf{x}}_0))] \\
& -n_z^{(k)}(z-z_0)E(m(\underline{\mathbf{x}};\underline{\mathbf{x}}_0))\} \\
& +(r+r_0)\left(1-m(\underline{\mathbf{x}};\underline{\mathbf{x}}_0)\right) \\
& \times\{\frac{n_r^{(k)}}{r}(z-z_0)(K(m(\underline{\mathbf{x}};\underline{\mathbf{x}}_0))-E(m(\underline{\mathbf{x}};\underline{\mathbf{x}}_0))) \\
& +\frac{1}{a(\underline{\mathbf{x}};\underline{\mathbf{x}}_0)+b(r;r_0)} \\
& \times[n_r^{(k)}(z-z_0)[(r-r_0)K(m(\underline{\mathbf{x}};\underline{\mathbf{x}}_0))-(r+r_0)E(m(\underline{\mathbf{x}};\underline{\mathbf{x}}_0))] \\
& +n_z^{(k)}[(r+r_0)^2E(m(\underline{\mathbf{x}};\underline{\mathbf{x}}_0))+(z-z_0)^2K(m(\underline{\mathbf{x}};\underline{\mathbf{x}}_0))]]\} \\
& -\frac{n_r^{(k)}(z-z_0)}{a(\underline{\mathbf{x}};\underline{\mathbf{x}}_0)+b(r;r_0)}\{(-\frac{1}{r_0})[(a(\underline{\mathbf{x}};\underline{\mathbf{x}}_0)-b(r;r_0)) \\
& +m(\underline{\mathbf{x}};\underline{\mathbf{x}}_0)\left(a(\underline{\mathbf{x}};\underline{\mathbf{x}}_0)-2r_0^2\right)] \\
& \times[(r-r_0)K(m(\underline{\mathbf{x}};\underline{\mathbf{x}}_0))-(r+r_0)E(m(\underline{\mathbf{x}};\underline{\mathbf{x}}_0))] \\
& +\frac{(a(\underline{\mathbf{x}};\underline{\mathbf{x}}_0)-2r_0^2)}{2r_0}[(r-r_0)E(m(\underline{\mathbf{x}};\underline{\mathbf{x}}_0))-(1-m(\underline{\mathbf{x}};\underline{\mathbf{x}}_0)) \\
& \times((r+r_0)E(m(\underline{\mathbf{x}};\underline{\mathbf{x}}_0))-2r_0K(m(\underline{\mathbf{x}};\underline{\mathbf{x}}_0)))]-(E(m(\underline{\mathbf{x}};\underline{\mathbf{x}}_0)) \\
& -K(m(\underline{\mathbf{x}};\underline{\mathbf{x}}_0)))((r-r_0)^2+(z-z_0)^2) \\
& -2E(m(\underline{\mathbf{x}};\underline{\mathbf{x}}_0))(a(\underline{\mathbf{x}};\underline{\mathbf{x}}_0)+b(r;r_0))\} \\
& +\frac{n_z^{(k)}}{2r_0}\{-4r_0(r-r_0)E(m(\underline{\mathbf{x}};\underline{\mathbf{x}}_0)) \\
& -\left(1-m(\underline{\mathbf{x}};\underline{\mathbf{x}}_0)\right)\left(a(\underline{\mathbf{x}};\underline{\mathbf{x}}_0)-2r_0^2\right) \\
& \times(E(m(\underline{\mathbf{x}};\underline{\mathbf{x}}_0))-K(m(\underline{\mathbf{x}};\underline{\mathbf{x}}_0))) \\
& +\frac{(z-z_0)^2}{a(\underline{\mathbf{x}};\underline{\mathbf{x}}_0)+b(r;r_0)} \\
& \times[(4r_0(r-r_0)-2(a(\underline{\mathbf{x}};\underline{\mathbf{x}}_0)-b(r;r_0)))(E(m(\underline{\mathbf{x}};\underline{\mathbf{x}}_0))-K(m(\underline{\mathbf{x}};\underline{\mathbf{x}}_0))) \\
& +m(\underline{\mathbf{x}};\underline{\mathbf{x}}_0)\left(a(\underline{\mathbf{x}};\underline{\mathbf{x}}_0)-2r_0^2\right) \\
& \times(2K(m(\underline{\mathbf{x}};\underline{\mathbf{x}}_0))-3E(m(\underline{\mathbf{x}};\underline{\mathbf{x}}_0)))]\}, \qquad \text{(A8)}
\end{aligned}
$$

and

$$
\begin{aligned}
& Y_6(\underline{\mathbf{x}};\underline{\mathbf{x}}_0;\underline{\mathbf{n}}^{(k)}) \\
= \; & [(1-m(\underline{\mathbf{x}};\underline{\mathbf{x}}_0)) + \frac{2m(\underline{\mathbf{x}};\underline{\mathbf{x}}_0)(z-z_0)^2}{a(\underline{\mathbf{x}};\underline{\mathbf{x}}_0)+b(r;r_0)}] \\
& \times\{\frac{n_r^{(k)}}{2r}[\left(a(\underline{\mathbf{x}};\underline{\mathbf{x}}_0)-2r^2\right)E(m(\underline{\mathbf{x}};\underline{\mathbf{x}}_0)) \\
& -(a(\underline{\mathbf{x}};\underline{\mathbf{x}}_0)-b(r;r_0))K(m(\underline{\mathbf{x}};\underline{\mathbf{x}}_0))] - n_z^{(k)}(z-z_0)E(m(\underline{\mathbf{x}};\underline{\mathbf{x}}_0))\} \\
& -(z-z_0)\left(1-m(\underline{\mathbf{x}};\underline{\mathbf{x}}_0)\right)\{\frac{n_r^{(k)}}{r}(z-z_0)(K(m(\underline{\mathbf{x}};\underline{\mathbf{x}}_0))-E(m(\underline{\mathbf{x}};\underline{\mathbf{x}}_0))) \\
& +\frac{1}{a(\underline{\mathbf{x}};\underline{\mathbf{x}}_0)+b(r;r_0)}\left(n_r^{(k)}(z-z_0)[(r-r_0)K(m(\underline{\mathbf{x}};\underline{\mathbf{x}}_0))\right. \\
& -(r+r_0)E(m(\underline{\mathbf{x}};\underline{\mathbf{x}}_0))] \\
& \left.+n_z^{(k)}[(r+r_0)^2E(m(\underline{\mathbf{x}};\underline{\mathbf{x}}_0))+(z-z_0)^2K(m(\underline{\mathbf{x}};\underline{\mathbf{x}}_0))]\right)\} \\
& -n_r^{(k)}\{2E(m(\underline{\mathbf{x}};\underline{\mathbf{x}}_0))(r-r_0)-\left(1-m(\underline{\mathbf{x}};\underline{\mathbf{x}}_0)\right)[(r-r_0)K(m(\underline{\mathbf{x}};\underline{\mathbf{x}}_0)) \\
& -(r+r_0)E(m(\underline{\mathbf{x}};\underline{\mathbf{x}}_0))] \\
& +\frac{(z-z_0)^2}{a(\underline{\mathbf{x}};\underline{\mathbf{x}}_0)+b(r;r_0)}[(3m(\underline{\mathbf{x}};\underline{\mathbf{x}}_0)(r+r_0)-2r)E(m(\underline{\mathbf{x}};\underline{\mathbf{x}}_0)) \\
& +(2r\left(1-m(\underline{\mathbf{x}};\underline{\mathbf{x}}_0)\right))K(m(\underline{\mathbf{x}};\underline{\mathbf{x}}_0))]\} \\
& +n_z^{(k)}(z-z_0)\{\frac{(z-z_0)^2}{a(\underline{\mathbf{x}};\underline{\mathbf{x}}_0)+b(r;r_0)}[(2-3m(\underline{\mathbf{x}};\underline{\mathbf{x}}_0))E(m(\underline{\mathbf{x}};\underline{\mathbf{x}}_0)) \\
& -2\left(1-m(\underline{\mathbf{x}};\underline{\mathbf{x}}_0)\right)K(m(\underline{\mathbf{x}};\underline{\mathbf{x}}_0))] + (3m(\underline{\mathbf{x}};\underline{\mathbf{x}}_0)-5)E(m(\underline{\mathbf{x}};\underline{\mathbf{x}}_0)) \\
& +3\left(1-m(\underline{\mathbf{x}};\underline{\mathbf{x}}_0)\right)K(m(\underline{\mathbf{x}};\underline{\mathbf{x}}_0))\}. \qquad \text{(A9)}
\end{aligned}
$$